

Investigation of Winglets and Drag Polars on a Cambered Eppler 212 Finite Wing

Zakary Steenhoek

This experiment aimed to investigate the lift and drag characteristics of a cambered Eppler 212 finite wing and to evaluate the impact of different winglet configurations on these aerodynamic properties. Using the ASU Flow-Visualization Tunnel, tests were conducted at Reynolds numbers of 150,000 and 300,000 to assess performance across a range of angles of attack. Results showed that the addition of winglets significantly influenced both lift and drag, with notable variations in performance depending on the winglet configuration. Comparative analysis highlighted the relationship between the aerodynamic efficiency and Reynolds number, emphasizing the importance of optimal winglet design for minimizing induced drag while maintaining or enhancing lift.

I. Nomenclature

ρ	=	air density
\mathcal{V}	=	volume
n	=	molar mass
R	=	universal gas constant
T	=	temperature
T_{ref}	=	reference temperature
U	=	internal energy
KE	=	kinetic energy
PE	=	potential energy
$C\mathcal{V}$	=	control volume
CS	=	control surface
\hat{n}	=	normal vector
∂	=	partial derivative
M	=	conversion factor
E	=	voltage
p_{atm}	=	atmospheric pressure
p_{∞}	=	dynamic pressure
V_{∞}	=	dynamic velocity
\dot{m}	=	mass time derivative
c	=	chord
b	=	span
S	=	planform area
α	=	angle of attack
C_L	=	lift coefficient
C_D	=	drag coefficient
L	=	lift
D	=	drag
F_A	=	normal force
F_N	=	axial force
μ	=	viscosity
μ_{ref}	=	reference viscosity
S_{μ}	=	Sutherland temperature
Re	=	Reynold number

II. Introduction

Drag and lift forces play a critical role in the performance and design of airfoils. These forces, and the relationship between them, are arguably some of the most important considerations for aerospace engineers to investigate when testing and designing an aircraft. It is known that the true drag force is a summation of multiple different components. This lab measured what can be considered as the total drag produced by a *finite* wing in steady flow, consisting of the pressure drag, friction drag, and induced drag. This is in contrast to previous experiments, where the induced drag component was considered negligible for an 'infinite' airfoil section. When working with finite wings, the induced drag component becomes significant, and absolutely must be considered for a complete analysis of wing behavior. This experiment aimed to measure and compare the complete lift and drag characteristics of a cambered Eppler 212 finite wing, and how various winglets and their configurations influence the lift-drag relationship.

Induced drag refers to the component of force acting against an aircraft or wing as a result of the lift that it produces. We know from the basic principal of lift that the dynamic pressure across the upper surface of a wing is lower than the dynamic pressure across the lower surface. This pressure differential exerts a force on the structure of the wing that acts to try and 'equalize' this pressure differential, and since high pressure always moves towards low pressure, this results in an upward force on the wing structure, a force that we call lift. When the structure is theoretically infinite, or when it is configured to act as infinite, this differential pressure only generates a lift force and pressure drag. However, when the structure is finite, as is the case with all practical application, this pressure differential results in an interaction of particular interest at the ends of the wing, where there is no physical structure separation. Physics does not yield, and the pressure differential still acts to equalize. As such, the high pressure zone underneath the wing flows *around* the ends of the wing to the low pressure zone above. This is the fundamental principal behind what is known as the wingtip vortex, and has considerable influence on the lift, drag, design, and performance of a wing. This wingtip vortex creates what is known as upwash and downwash. Upwash is the upward velocity induced from the wingtip vortex, and as you might expect, occurs beyond the span of the wing. Downwash is the downward velocity induced from the wingtip vortex, and occurs throughout the area underneath the span of the wing. Downwash effectively tilts the relative flow downwards, which means the wing is effectively at a slightly lower angle of attack than the pure geometric angle of attack. The opposite is true for upwash.

The negative effects of wingtip vortices can be influenced by placing structures at the ends of the wing which act to 'block' the induced velocity from pressure equalizing around the wing. These structures are called winglets. The addition of winglets is known to alter the wingtip vortex in a way that can be thought of as making the radius of the vortex larger, as the air must travel a further distance to reach the low pressure on top of the wing, reducing induced drag and downwash, and potentially enhancing lift. As stated, this lab aims to investigate the impact of winglets, and tests various different configurations. Each configuration belongs to one of three 'families': location, length, or angle. Within each family, there are three different configurations. The location family configurations are front, back, and middle, referring to where along the chord the wingtip is placed. The length family configurations are small, medium and long, and refer to the proportion of chord spanned by the wingtip. The angle family consists of 20, 40, and 60 degrees, and refer to the angle the wingtip makes with the plane of the chord. Tests were also conducted without a winglet to provide a reference for analysis. All 10 of these configurations were tested at a Reynold number of 150,000 and 300,000 to analyze the impact of these winglets in different flow conditions. The 'ideal' winglet would combine characteristics from each family to provide the greatest increase in performance and efficiency compared to a wing without any winglet.

The wing used in this experiment is constructed from Eppler 212 airfoil sections. The Eppler 212 is considered to be a supercritical airfoil. Airfoils considered to be supercritical are often characterized by a flatter upper surface near the mid-chord with significant camber in the aft portion, and a larger leading edge radius. This design aims to delay the formation of shock waves and wave drag at transonic speeds by pushing the shock further aft. This results in an improved lift-to-drag ratio and a higher critical mach number, but requires careful design of control surfaces and a stronger control system. For the purposes of this experiment, the Eppler 212 wing will be tested in low-speed flow conditions.

In summary, the objective of this experiment is to investigate the lift and drag characteristics of an Eppler 212 finite wing section in low-speed turbulent flow conditions, and how the addition of wingtip devices impact these characteristics and the relationship between them, in order to theorize an ideal wingtip configuration that will reduce the negative effects of wingtip vortices, increase lift, and reduce induced drag to provide a more efficient wing section.

A. Assumptions

Critical assumptions are made in this experiment which make it possible to produce meaningful results without creating substantial error. These assumptions allow for simplicity in data collection and processing, and permit the use

of some key physical laws. Assumptions made include the following:

1. Ideal Atmosphere

To determine the density of the laboratory air, the ideal gas law is used, which is only applicable to ideal gasses. The assumption is made that the atmosphere may be treated as an ideal gas.

2. Incompressible & Uniform Flow

Methods to determine flow velocity through the test area apply the conservation of mass. The fluid flow is assumed to be uniform, and density of laboratory air is assumed to be constant, and therefore the term representing the change in mass inside the control volume w.r.t time evaluates to zero.

B. Physical Laws

1. Ideal Gas Law

The first governing law in this experiment fundamental ideal gas law, Eq. (1). This is a thermodynamic equation of state for an ideal gas, which relates physical properties and known constants.

$$pV = nRT \quad (1)$$

2. Bernoulli's Equation

The next governing law is the fundamental conservation of energy equation, Eq. (2), which states that the total energy of a system, consisting of the internal energy U , the kinetic energy KE , and the potential energy PE , remains constant.

$$U + KE + PE = const. \quad (2)$$

3. Mass Conservation

The next governing law is the fundamental conservation of mass, Eq. (3), which states that the change in mass inside a control volume w.r.t time plus the mass convected across the control surface must always sum to 0.

$$\frac{\partial}{\partial t} \int_{CV} \rho dV + \int_{CS} \rho (\vec{V} \cdot \hat{n}) dA = 0 \quad (3)$$

4. Error Propagation

The final governing equation is Gauss's formula for error propagation, Eq. (4), which describes the effect of uncertainty in a calculation as a function of the uncertainty in the variables involved, where i is the number of variables with uncertainty.

$$\delta y = \sqrt{\sum_i \left(\frac{\partial y}{\partial x_i} \delta x_i \right)^2} \quad (4)$$

III. Procedure

A. Experimental Equipment

1. ASU Flow-Visualization Tunnel

The tunnel used in this experiment (1) is a low-speed in-draft style tunnel, which draws outside air through a screening system to improve and idealize the flow. It has an octagonal test section with a slight taper to account for boundary-layer growth, and a contraction area ratio of 25:1. An external force balance is mounted inside the test section to measure aerodynamic forces and moments of the model inside. The streamwise flow characteristics are determined based on an input Reynold number. A diagram is shown in Fig (1)

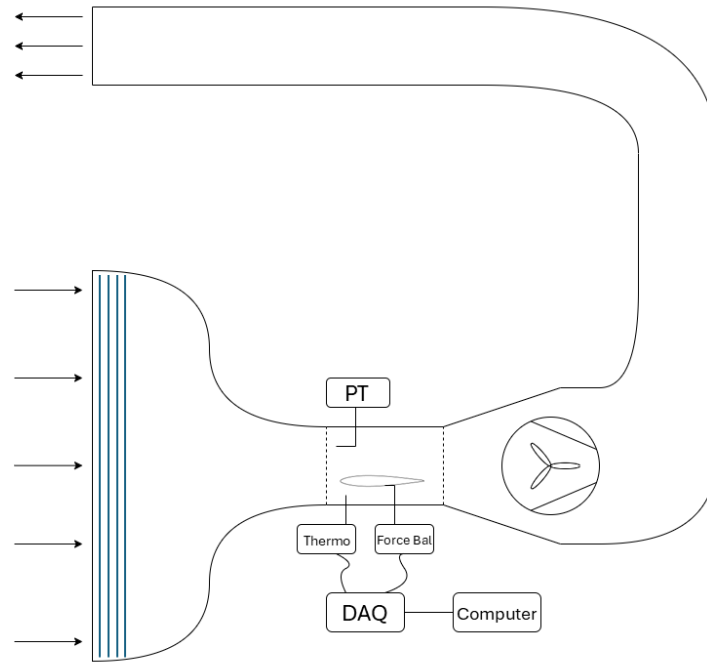


Fig. 1 Schematic of the wind tunnel setup used for data collection, including the related sensing devices and data acquisition method

2. Eppler 212 finite airfoil

The Eppler 212 airfoil is a supercritical airfoil section that has a large leading edge radius and aftward maximum camber. It produces meaningful lift across a very wide range of pitch angle, making it suitable for high angle of attack applications. This experiment uses a rectangular, untwisted planform consisting of uniform Eppler 212 airfoil sections.

3. Digital thermocouple

A digital thermocouple[2] is a digital measurement device that measures temperature, displayed in degrees Celsius. The device consists of two conductors of different metals - the hot and the cold junction. When the hot junction is heated, it generates a voltage proportional to the temperature difference between the plates. This measurement is integral to determining the density of the atmosphere inside of the lab.

4. Pressure transducer

The pressure transducer works in a similar way to the absolute pressure transducer described above, but measures the difference between two pressure values, and writes a proportional output in volts. One side of this device reads the stagnation pressure, while the other side reads the static pressure. The measurement obtained from this device is a gauge pressure.

5. Pitot tube

A pitot tube[3] is a physical tube-shape object with a central hole down the length of the tube and several holes drilled around the outside of the tube. These holes are kept separate, and the pressure transducer is connected across these holes to read the difference, i.e. the dynamic pressure. This is the device connected to the pressure transducer. There is a 90 degree bend present to normalize any disrupting airflow inside the tube.

6. Force Balance

A force balance is an instrument used to measure the aerodynamic forces on a model during testing. There are various different kinds, but the two main types are internal and external balances. For this lab, an external force balance was used, to which the Eppler 212 wing section is attached. This allows measurement of the normal and axial forces experienced by the wing during testing. It uses load cells, which convert physical forces into a signal output by measuring the pressure induced as a result of loading forces, from which the signal is recorded.

7. Data Acquisition System (DAQ)

The data acquisition system, or DAQ, is a system that connects measurement devices and instruments to a computer running a data acquisition software[4]. It is used to convert and record the signal output from all of the instruments used during testing, and prepares it to be analyzed by engineers. The DAQ is connected to a computer running a data acquisition software, which processes and stores the instrument readings. Often times, this processing involves signal conditioning, filtering, and analog-to-digital conversion to record and output usable data.

B. Data Collection

1. Part 1: Ambient Air Pressure and Density

For the first part of the data collection, the ambient air density must be determined prior to each configuration test. This is done by taking measurements of the absolute pressure and the temperature inside the wind tunnel, using the pressure transducer and digital thermocouple, respectively. The governing equation here is the fundamental ideal gas law, Eq.(1), which relates pressure, volume, temperature, matter, and the universal gas constant. This equation can be rearranged and simplified by expanding the term representing matter into m/M , introducing density as m/V , and defining the specific gas constant as R/M as seen in Eq.(5).

$$p = \frac{m}{V} \frac{R}{M} T \quad (5)$$

The result is Eq.(6), which relates pressure, density, and temperature with a known constant value specific to air.

$$p = \rho RT \quad (6)$$

This equation can then rearranged to solve for ρ as a function of p and T , seen in Eq.(7).

$$\rho = \frac{p}{RT} \quad (7)$$

The error associated with this measurement is found using Eq.(8), derived from Eq.(4), the partial derivatives of Eq.(7) w.r.t. p and T , and the known machine errors, δp and δT .

$$\delta \rho = \sqrt{\left(\frac{1}{RT} \delta p\right)^2 + \left(\frac{p}{RT^2} \delta T\right)^2} \quad (8)$$

2. Part 2: Wind Tunnel Testing

Before collecting any data, the dimensions of the Eppler 212 wing must be obtained. The chord and span were recorded as 0.1397m and 0.1524m, respectively. As mentioned above, the ambient air pressure and temperature are to be measured at this point. The wing, *without* any winglet configuration, is then mounted in the test section, and is adjusted such that the geometric angle of attack is zero degrees. To obtain accurate lift and drag measurements, the weight of the wing must be considered. To measure this, the normal and axial forces are recorded from negative fifteen degrees to positive twenty degrees with the wind tunnel turned off. Without any wind speed, there are no forces on the airfoil except its weight, and as such, these values represent only the gravitational contributions to the normal and axial forces. These values will be considered in data processing to obtain accurate lift and drag. Next, the wind tunnel is set to a Reynolds number of 150,000, and all sensor and instrument measurements are taken roughly every degree from negative fifteen to positive twenty. The wind tunnel is then set to a Reynolds number of 300,000, and once again, data is collected every degree between negative fifteen and positive twenty. This procedure will produce three data files for each winglet configuration to be saved and exported for analysis.

The procedure described above, excluding measuring dimensions, should then be performed for every winglet configuration. In order to make any meaningful comparison or conclusion about the effects of wingtips, there needs to be attention to detail to reduce error and preserve repeatability. Gravity data needs to be measured every time, as adding winglets will make a non-negligible contribution. Ambient air measurements also need to be taken prior to every test, as these are important for determining accurate coefficients, and ambient conditions can fluctuate in the minutes between tests. Particularly the temperature, as the in-draft setup of the wind tunnel draws from outside air, which is more susceptible to the daily temperature high/low cycle.

3. Part 3: Drag and Lift Calculations

The following procedures for calculations are common for every test conducted, as the data collection procedure does not change, and as such, neither do the steps for extracting the desired values. First, the normal and axial force data from the gravitational tests are subtracted from the normal and axial force data from the associated tests at Reynold numbers of 150,000 and 300,000. This yields force values that solely represent the resultant body forces due to the incoming flow. Next, the axial and normal body forces are projected onto the wind axes, using the trigonometric relationships below in Eq.9 and Eq.10.

$$L = F_N \cdot \cos \alpha - F_A \cdot \sin \alpha \quad (9)$$

$$D = F_N \cdot \sin \alpha + F_A \cdot \cos \alpha \quad (10)$$

To determine the lift and drag coefficients, the lift and drag forces must be made non-dimensional by dividing by dynamic pressure times planform area. The planform area is constant, and simply found as the product of chord and span, measured in the beginning of the experiment. The dynamic pressure must be calculated using the known Reynold number, pressure, and temperature. The Reynold numbers for each configuration are recorded more exactly alongside the pressure and temperature, and can be found in the conditions file. Density is calculated first, as described in part 1. Next, Sutherland's law is used to determine the dynamic viscosity as a function of temperature. Sutherland's law, seen in Eq.11 is used to relate the absolute temperature of an ideal gas to the dynamic viscosity at that temperature[5].

$$\mu = \mu_{ref} \left(\frac{T}{T_{ref}} \right)^{3/2} \left(\frac{T_{ref} + S_\mu}{T + S_\mu} \right) \quad (11)$$

Where $\mu_{ref} = 1.716E^{-5} kg/ms$, $T_{ref} = 273.15K$, and the Sutherland temperature $S_\mu = 110.4K$, constant for ideal air. Next, the flow velocity can be calculated as a function of the known Reynold number, and the calculated viscosity and density, seen below in Eq.12

$$Re = \frac{\rho V_\infty c}{\mu} \quad (12)$$

Finally, the dynamic pressure can be obtained using the known formula, seen below in Eq.

$$p_\infty = \frac{1}{2} \rho V_\infty^2 \quad (13)$$

Using the computed dynamic pressure, the lift and drag force can be made dimensionless as stated above by the equations below, Eq.14 and Eq.15

$$C_L = \frac{L}{q_\infty S} \quad (14)$$

$$C_D = \frac{D}{q_\infty S} \quad (15)$$

4. Part 4: Uncertainty Calculations

We know laboratory measurements are not, and can not be perfectly accurate. Thus, some uncertainty is induced through the calculations performed to obtain the lift and drag coefficient. This uncertainty can be derived from Eq.4, where all values required to obtain the lift and drag coefficient, except the planform area, carry some amount of error, either from calculation from other measured values, or from the known machine error. The force balance carries a known amount of error, δF_N and δF_A , equal to five-hundredths of a newton. The measured geometric angle of attack, α , carries a known error $\delta \alpha$ of five-hundredths of a degree. The final variable with uncertainty is the dynamic pressure.

This uncertainty is propagated from the flow velocity and density, both of which are also calculated values, carrying their own uncertainty, and so on. This quickly becomes a monotonous computation, and the uncertainty in dynamic pressure can be averaged to a constant of half a pascal. Then, the uncertainty in lift and drag coefficient can be determined using Eq.16 and Eq.17.

$$\delta C_L = \sqrt{\left(\frac{\partial C_L}{\partial F_A} \delta F_A\right)^2 + \left(\frac{\partial C_L}{\partial F_N} \delta F_N\right)^2 + \left(\frac{\partial C_L}{\partial \alpha} \delta \alpha\right)^2 + \left(\frac{\partial C_L}{\partial q_\infty} \delta q_\infty\right)^2} \quad (16)$$

$$\delta C_D = \sqrt{\left(\frac{\partial C_D}{\partial F_A} \delta F_A\right)^2 + \left(\frac{\partial C_D}{\partial F_N} \delta F_N\right)^2 + \left(\frac{\partial C_D}{\partial \alpha} \delta \alpha\right)^2 + \left(\frac{\partial C_D}{\partial q_\infty} \delta q_\infty\right)^2} \quad (17)$$

C. Data Processing

For data processing, it will yield beneficial to split the code into a few different scripts and functions. The first step is to read, clean up, and store all of the data, and to ensure it is in an expected configuration. The MATLAB software is used throughout to program processing methods and present the data. Read the files from a folder, and parse the titles to determine what is contained within. The conditions file is read in first and separately to obtain a list of all wingtip configurations. Each file name is split and the substrings are examined to identify each gravity data file, and each specific test file at both Reynolds numbers. A descriptive short name is pieced together, and structured with the trimmed data array.

With all the data in a uniform and accessible format, The main loop is constructed to extract the related conditions and gravity data for every test file and pass it into an external function. This function performs all computations explained above, ensuring gravitational correction, angle conversion to radians, and symbolic to numerical differentiation for all uncertainty calculations. Returned to the main loop are the pressure, pressure uncertainty, pitch angle, lift and drag coefficients, and uncertainty in the lift and drag coefficients. The processed data is stored before the loop iterates again over the next test file. Once all 20 files have been processed, a sorting algorithm is executed to create data sub-structures corresponding to each data plot seen later in the results. Finally, each of these sub-structures are passed into a plotting function, which creates a lift-curve C_L vs. α plot, and a drag polar C_D vs. C_L plot. These plots were created for each family at both Reynold numbers, and plotted with the data for the wingtip-less test, for a total of 12 graphics. The Full processed data structure is also exported to an excel sheet for table presentation.

IV. Results

The 12 plots are presented below:

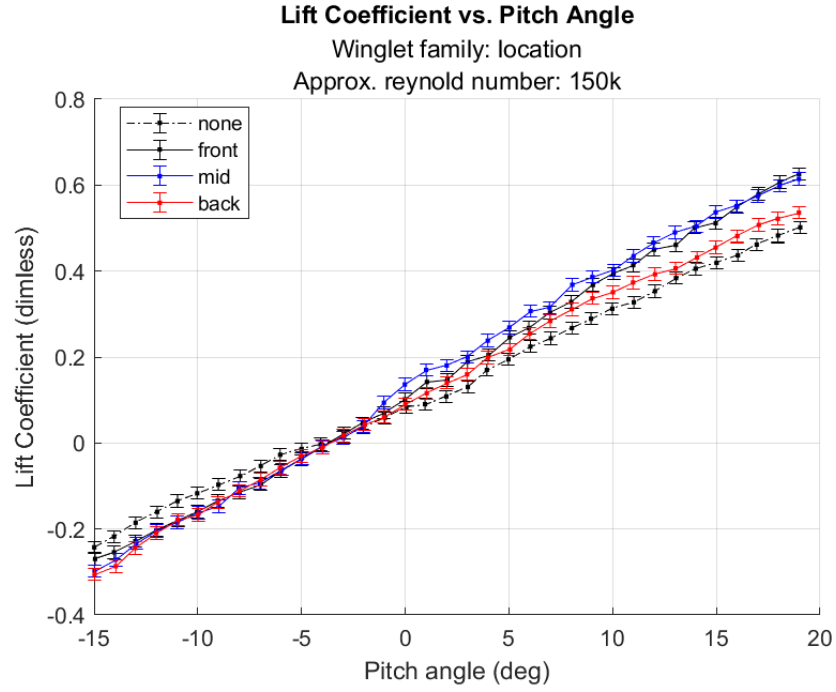


Fig. 2 C_L vs. α for the location family and no winglet at $Re = 150,000$

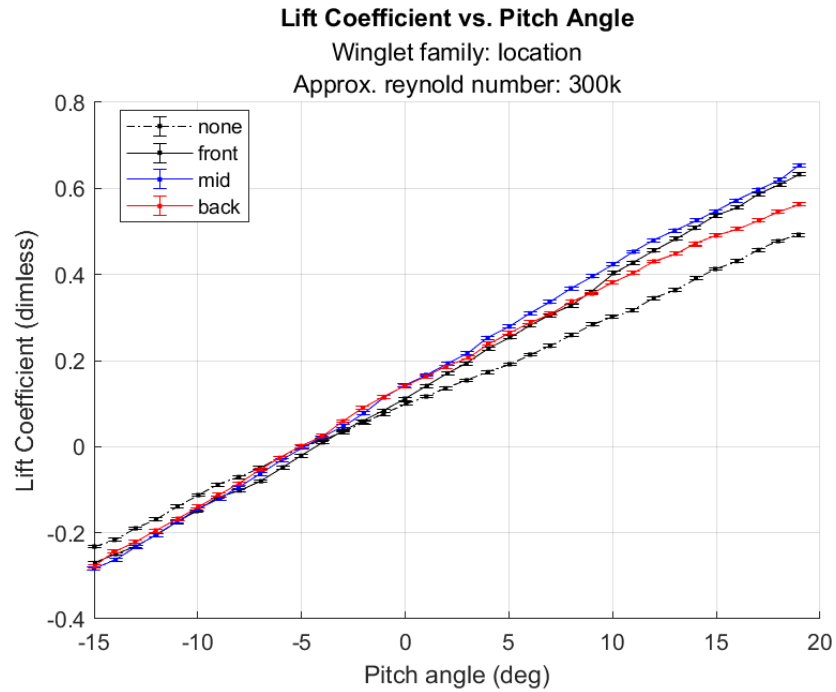


Fig. 3 C_L vs. α for the location family and no winglet at $Re = 300,000$

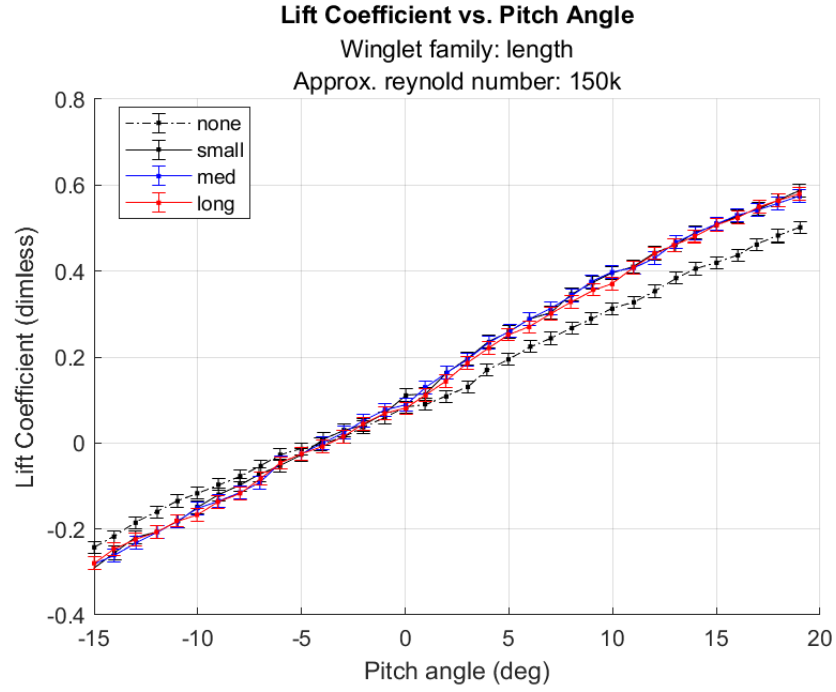


Fig. 4 C_L vs. α for the length family and no winglet at $Re = 150,000$

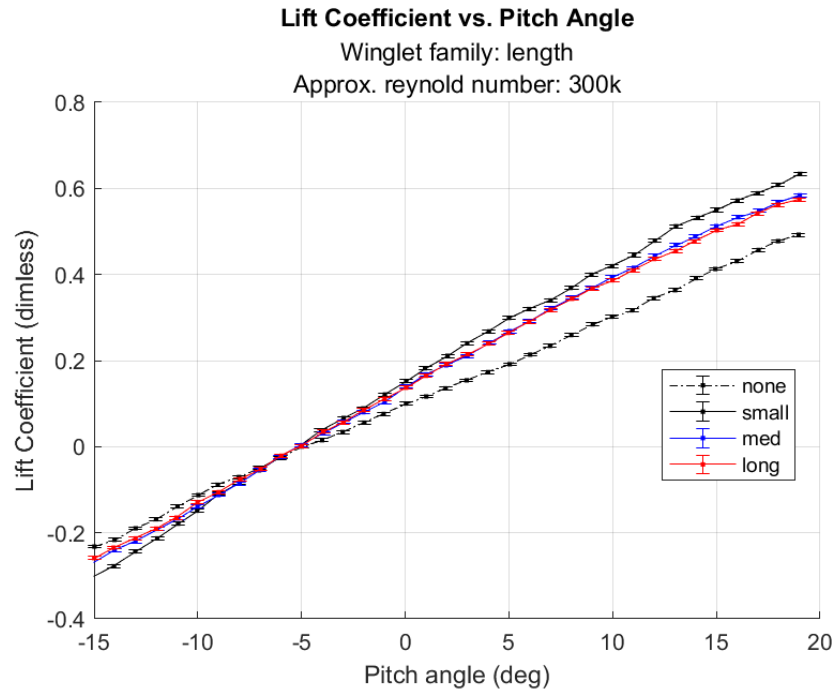


Fig. 5 C_L vs. α for the length family and no winglet at $Re = 300,000$

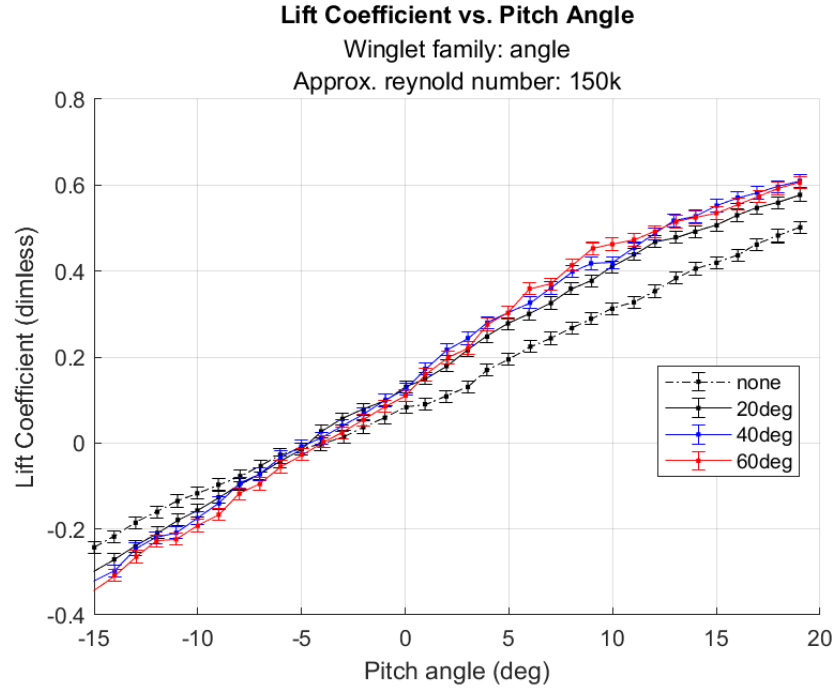


Fig. 6 C_L vs. α for the angle family and no winglet at $Re = 150,000$

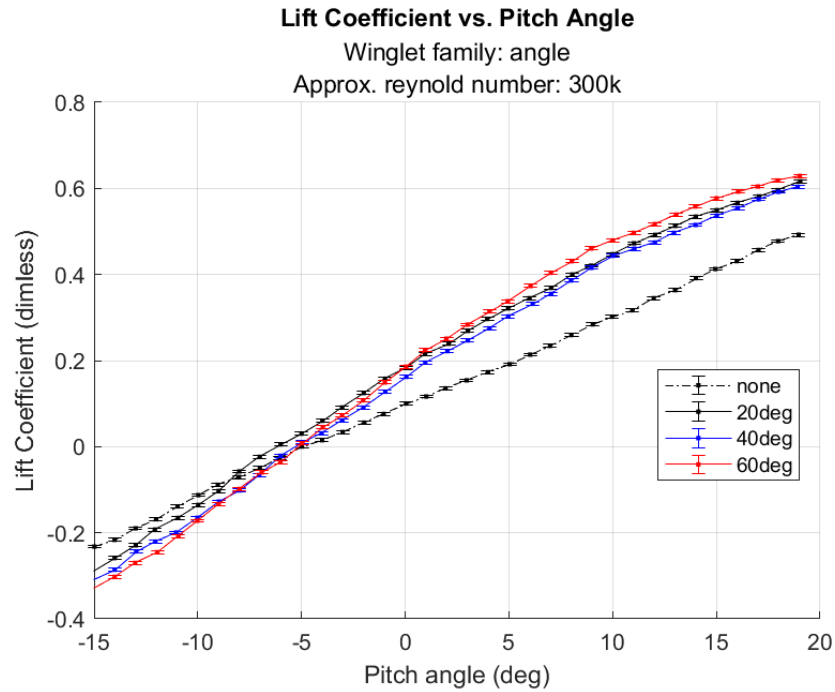


Fig. 7 C_L vs. α for the angle family and no winglet at $Re = 300,000$

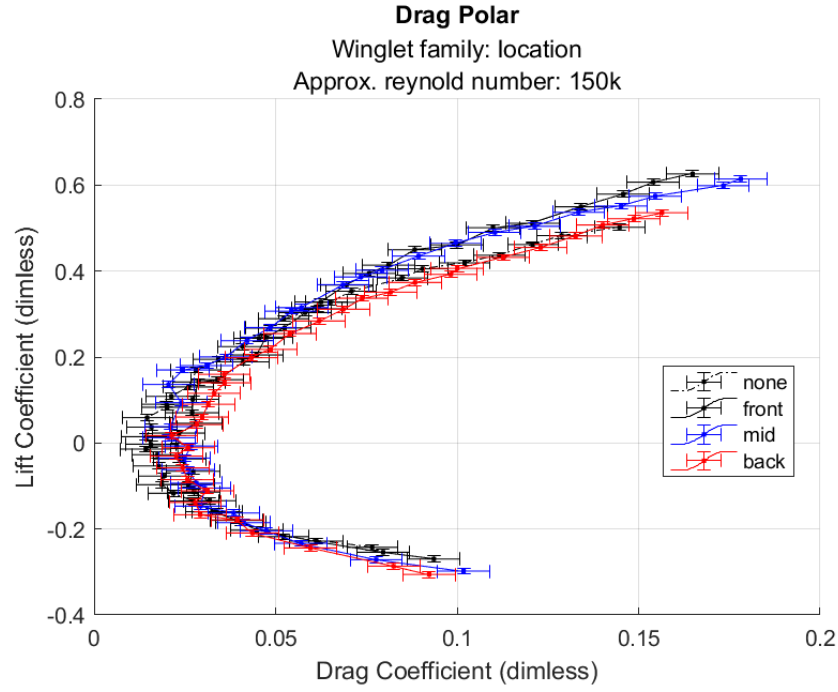


Fig. 8 C_L vs. C_D for the location family and no winglet at $Re = 150,000$

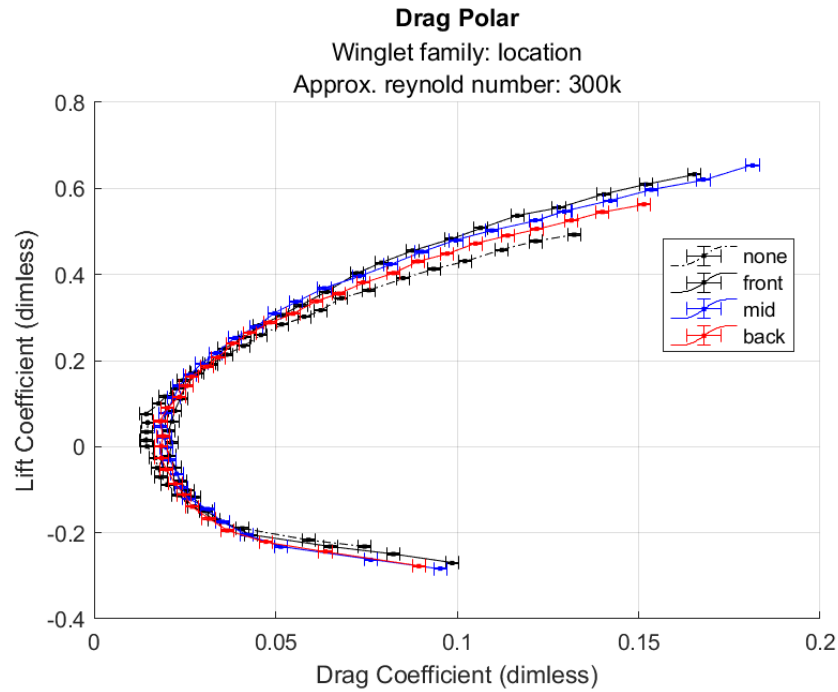


Fig. 9 C_L vs. C_D for the location family and no winglet at $Re = 300,000$

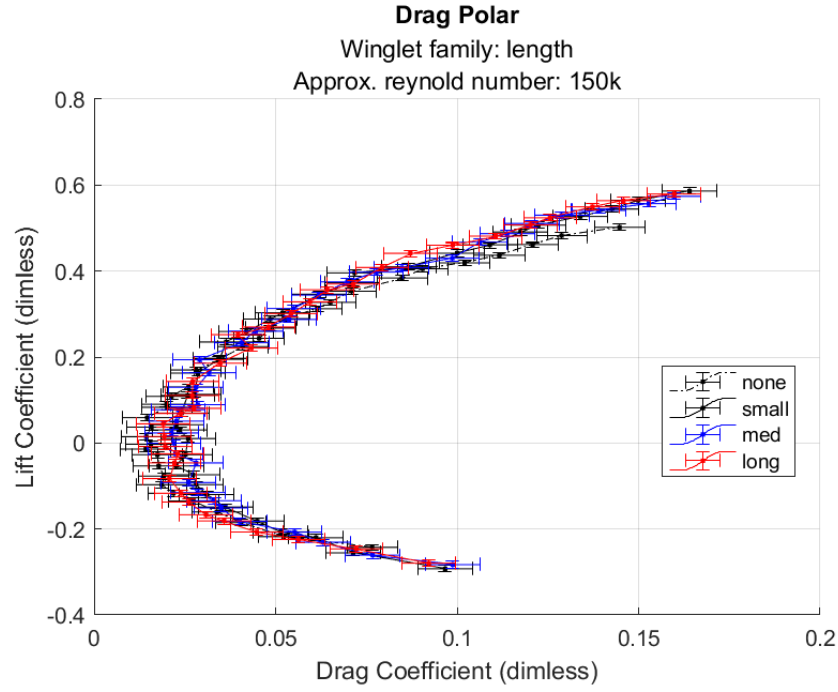


Fig. 10 C_L vs. C_D for the length family and no winglet at $Re = 150,000$

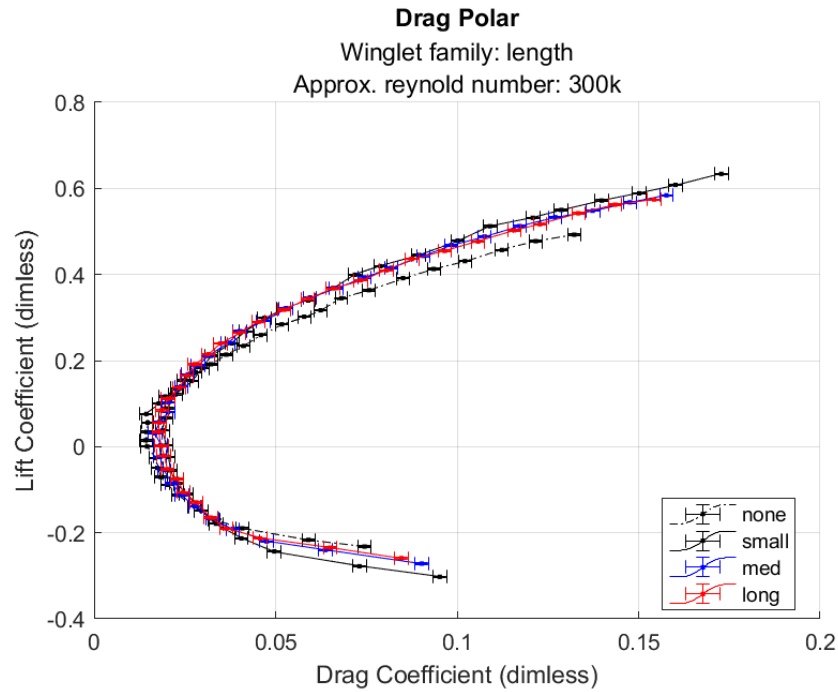


Fig. 11 C_L vs. C_D for the length family and no winglet at $Re = 300,000$

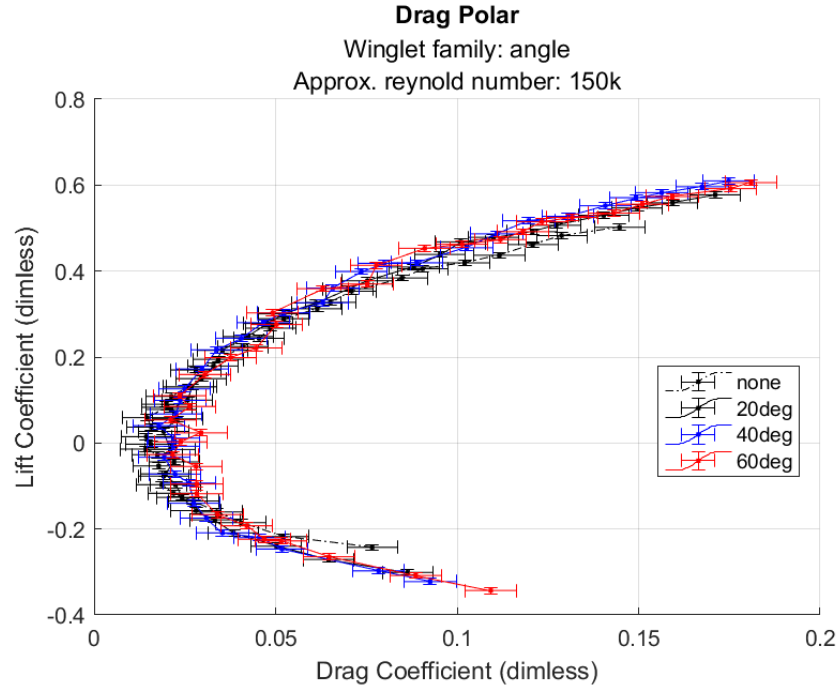


Fig. 12 C_L vs. C_D for the angle family and no winglet at $Re = 150,000$

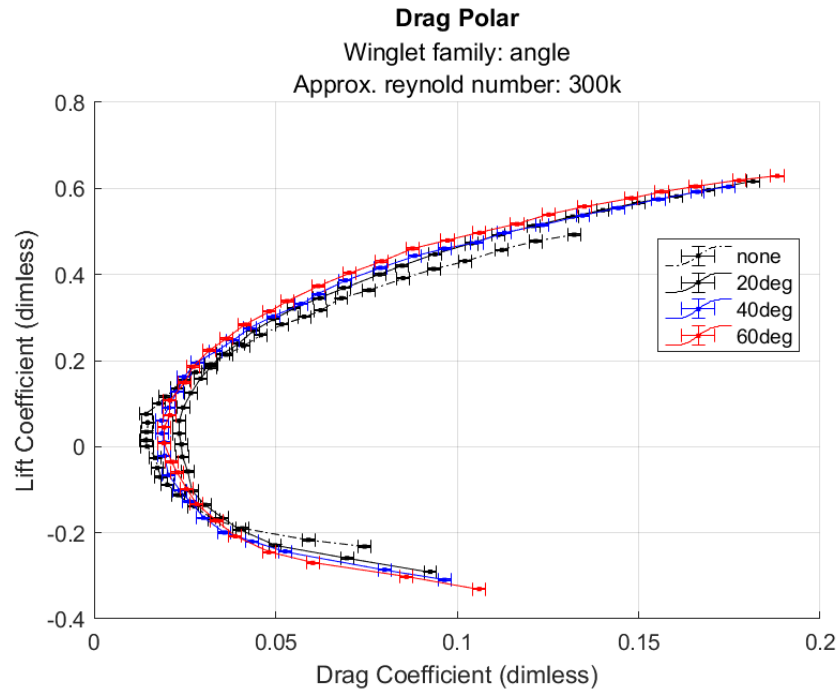


Fig. 13 C_L vs. C_D for the angle family and no winglet at $Re = 300,000$

First, an analysis of Fig 2-Fig 6. The most glaring trend is that the lift-curve slope for every single winglet configuration is higher than the lift-curve slope for the winglet-less configuration, plotted consistently throughout as the black dashed line. Thus, a definitive conclusion can be made that the installation of *any* wingtip device tested will result

in the wing section providing more lift throughout the entire range of pitch.

An analysis of the drag polar plots yields another glaring trend. Each of them show that the configuration with smallest minimum drag coefficient is one without any winglet device. Knowing that the drag coefficient is a sum of pressure, friction, and induced drag, the minimum value must be obtained when each of those components are minimized. The figures show that this happens when the lift coefficient is approximately zero. When the airfoil is generating zero lift, it will not generate wingtip vortices, and thus will experience no induced drag. Also at zero lift, there is no upward lifting force due to the upper and lower surface pressure differential, but there may still be a component of streamwise drag force due to pressure differential in the streamwise direction. This is likely a relatively small contribution, but is due to things like the camber, thickness, and angle of attack, and can be simply called form drag. The frictional drag component does not change as a function of lift, as it is a result of the interaction between the viscous forces and the wing surface. Since we are testing at constant Reynolds numbers, this can be assumed to be a constant for each winglet-Reynold configuration. All that is to say that the configuration with the smallest minimum drag coefficient has the smallest frictional and form drag. This makes sense, as any winglet will add more surface area for viscosity interaction, and as well more 'form' for streamwise pressure differential to develop. Thus, the addition of any winglet will introduce more 'permanent' drag, although the graphs show that this increase is marginal at best. The drag polar plots also show, however, that the no-winglet curve appears 'stretched', and as the wing begins to generate lift, this curve will intersect the winglet configuration curves. After this intersection, which occurs at $C_L \approx 0.2$ for the 150,000 Reynold number tests and $C_L \approx 0.15$ for the 300,000 Reynold number tests, the no-winglet configuration has a lower magnitude $\frac{C_L}{C_D}$ ratio. This is an indication of a less efficient configuration, as it produces less lifting force for the same drag force experienced.

Essentially, analysis of the drag polar plots shows that the addition of winglets causes an aggregate increase in form and frictional drag, but also an increase in lifting efficiency and a *significant* decrease in induced drag, which quickly becomes the dominant drag force as lift is produced.

Next, an analysis of the influence Reynold's number on the lift coefficient and drag coefficient. Foremost, there is clearly a jarring difference in data uncertainty between the two tested Reynolds numbers. At a constant pressure, temperature, and chord, the Reynold number increases linearly with the free stream velocity, i.e. the airspeed at the 300,000 tests is double that of the airspeed at the 150,000 tests. Thus, the higher speed increases steady-state stability and produces more certain measurements. Still, however, a qualitative analysis may be made. The lift-curve plots show that the zero-lift angle is higher at a lower Reynold number, and visa versa. This is particularly apparent in Fig 4 and Fig 5, where the zero lift angles are roughly negative four degrees and negative five degrees, respectively. This translates a greater C_L at a higher Reynold number. However, a similar analysis of the drag polar plots indicates a higher C_D at a higher Reynold number.

The range of data collected in this experiment does not allow for a fair or conclusive analysis of the effects of winglets or Reynold number on stall characteristics. However, what has discovered thus far and what is known about and the Reynold number permits some theoretical analysis. A higher Reynold number indicates turbulent flow, and higher flow energy. This causes the air to 'stick' to the airfoil more, and flow separation, which induces stall, is harder to achieve. Winglets work to mitigate the effects of the wingtip vortex, which is known to cause spanwise flow as the low pressure air travels over the wingtips. Spanwise flow tends to destabilize the streamwise flow and the boundary layer near the wingtips, which can make these areas more prone to flow separation. The wingtip devices may contribute a slight increase in stall angle, but this is not their primary function.

One last note about the lift-curve slopes. The thin airfoil theory states that the lift coefficient will increase by about 0.11 for every one degree inclination in pitch. A quick analysis of the lift curve slopes presented here show that this does not hold. Looking at Fig 5, where the zero-lift angle is negative five degrees, a five degree pitch increase causes a lift coefficient increase of approximately 0.15 for the winglet family and 0.1 for the bare wing. According to thin airfoil theory, a 5 degree increase should cause a lift coefficient increase of approximately 0.55. This is expected, as finite wing analysis shows that the lift-curve slope for finite wings is scaled down as a function of aspect ratio and conversion factor τ .

V. Conclusion

The experiments performed in this lab support the theories presented in the introduction. The addition of winglet devices are seen to increase the lift coefficient and reduce the induced drag coefficient. While the addition of winglets does increase the frictional and form drag, this increase is nearly negligible, and is quickly rendered insignificant with respect to the induced drag as lift is generated.

Family-specific expectations can be derived from engineering intuition and what is traditionally seen in real-world practice. The traditional winglet, as seen on commercial and transport jets, typically has a vertical or nearly-vertical angle, is slightly swept, and spans the entire tip chord length. This design is intuitively sound, considering what is known about the effects of finite wing design, the wingtip vortex, and downwash. A high angle relative to the spanwise plane means the air flowing to low pressure must take a longer path, increasing the vortex radius, and reducing the intensity of the downwash. This high inclination across the entire tip chord leaves no available space for the flowing air to bypass the winglet, so it all *must* go around the winglet. The backward winglet sweep increases aerodynamic efficiency and reduces form drag, just as with a swept wing. The backward sweep also works to shift wingtip vortex formation as far behind the wing as possible, further reducing the influence of downwash and induced drag.

The experimental data collected supports these hypotheses within reason. Most wingtips in practice are implemented on swept and tapered wings, where the tip chord is 'small'. The length data at a Reynold number of 300,000 shows the small configuration to provide the greatest lifting benefit, however the 150,000 data shows that length is relatively insignificant. The angle lift curve slope data supports the expectation that a high inclination mitigates the wingtip vortex to a greater degree, as the angle data at a Reynold number of 300,000 shows that the 60 degree configuration provides the greatest benefit. Finally, the lift curve data from the location family at a Reynold number of 300,000 shows that a front or middle configuration provides the greatest benefit. This does not directly support real-world implementation, where location cannot really be considered for a winglet spanning the tip cord entirely, however previous laboratory experiments have shown that the forward portion of an airfoil generates a greater pressure differential, so the magnitude of vortex generation should be greater. Thus, placing the winglet device further fore will result in greater vortex mitigation. These conclusions are supported by the overall drag polar plot data as well. The aforementioned 'ideal' configurations typically have the higher lifting efficiency, i.e. they are more effective at mitigating the wingtip vortex, mitigating the effects of downwash, and reducing induced drag. One area to investigate further is the addition of a second winglet, with this ideal configuration, extending downward from the tip chord. This would increase the physical distance the flow must take to travel to the low pressure zone and even further increase the vortex radius, and would introduce a second winglet vortex. The lower and upper winglet vorticies would both rotate in the same direction, meaning that the air at the *top* of the lower vortex is moving in the opposite direction as the air at the *bottom* of the upper vortex, mitigating the induced velocity in the space between, and potentially further reducing downwash and induced drag.

One big area of improvement to explore in this experiment is the data acquisition. Some of the data files were incredibly noisy, sporadic, and unusable. This meant cherry picking and manually cleaning data to produce any meaningful output. The DAQ could be updated to detect, prevent, or manage this through better signal processing methods. The physical sensors may also need to be cleaned, adjusted, tuned, or flat out replaced. This would reduce error and provide more dependable and repeatable results.

A. Appendix A: Tabulated Data

Wingtip	ρ	$\delta\rho$
none	1.14126	0.0040401
20deg	1.14052	0.0040364
40deg	1.15413	0.0041223
60deg	1.15303	0.0041131
small	1.18230	0.0042835
med	1.17869	0.0042566
long	1.17006	0.0041975
front	1.16585	0.0041707
mid	1.16001	0.0041387
back	1.16036	0.0041441

Table 1 Table A-1: Density and associated uncertainty. Measured prior to testing of each winglet configuration.

$\alpha(150k)$	$C_L(150k)$	$\delta C_L(150k)$	$\alpha(300k)$	$C_L(300k)$	$\delta C_L(300k)$
-15.042	-0.30096	0.013843	-15.047	-0.29054	0.003489
-14.028	-0.27078	0.013837	-14.012	-0.25888	0.003487
-13.003	-0.24	0.013832	-12.99	-0.2292	0.003486
-11.95	-0.20917	0.013828	-12.066	-0.19264	0.003484
-10.965	-0.17878	0.013824	-10.954	-0.16561	0.003483
-10.022	-0.15717	0.013822	-9.9793	-0.1352	0.003483
-8.9977	-0.12643	0.013819	-8.9941	-0.10293	0.003482
-8.0037	-0.096953	0.013817	-8.0012	-0.057636	0.003481
-7.0236	-0.071815	0.013816	-7.0089	-0.023753	0.003481
-6.0213	-0.043944	0.013815	-6.0094	0.00545	0.003481
-4.9975	-0.015061	0.013814	-5.0002	0.030378	0.003481
-4.0554	0.027024	0.013814	-3.9942	0.060247	0.003481
-3.0271	0.056059	0.013815	-3.0367	0.091055	0.003482
-2.0083	0.078113	0.013816	-1.9983	0.12456	0.003482
-0.9464	0.099795	0.013817	-0.96785	0.15779	0.003483
0.041263	0.13075	0.013819	0.042441	0.18341	0.003484
0.95287	0.14975	0.013821	0.95757	0.21531	0.003485
1.99	0.17913	0.013824	2.0894	0.23917	0.003486
3.0138	0.21572	0.013829	3.0115	0.26898	0.003487
3.9454	0.24748	0.013833	3.9505	0.2965	0.003488
4.9549	0.27819	0.013838	4.957	0.32132	0.00349
5.9676	0.30046	0.013842	5.996	0.34501	0.003491
7.0273	0.32563	0.013847	7.0331	0.36881	0.003492
7.9806	0.35902	0.013854	8.0613	0.40008	0.003494
8.9866	0.37736	0.013859	8.9568	0.42056	0.003496
9.9737	0.4095	0.013867	9.9953	0.44685	0.003498
11.026	0.4388	0.013874	11.035	0.4724	0.0035
12.045	0.46805	0.013883	12.049	0.49199	0.003501
13.041	0.47857	0.013886	13.005	0.51295	0.003503
13.985	0.49151	0.01389	14.009	0.53434	0.003505
15.014	0.50653	0.013895	15.022	0.54922	0.003507
15.994	0.52979	0.013902	16.023	0.56641	0.003509
16.953	0.54687	0.013908	17.062	0.58126	0.003511
17.979	0.55892	0.013912	17.974	0.59612	0.003512
19.031	0.57731	0.013919	19.041	0.61608	0.003514

Table 2 Table A-2: C_L vs. α plot data, 20 degree wingtip configuration

$\alpha(150k)$	$C_L(150k)$	$\delta C_L(150k)$	$\alpha(300k)$	$C_L(300k)$	$\delta C_L(300k)$
-15.02	-0.32247	0.01433	-15.02	-0.30959	0.00359
-14.006	-0.29747	0.014325	-14.007	-0.28591	0.003588
-12.999	-0.24669	0.014315	-12.97	-0.24321	0.003586
-12.022	-0.22018	0.014311	-12.039	-0.22055	0.003585
-11.044	-0.20881	0.01431	-11.04	-0.19946	0.003584
-10.018	-0.17475	0.014306	-10.016	-0.1653	0.003583
-8.9768	-0.14024	0.014302	-8.975	-0.12749	0.003583
-7.9402	-0.093226	0.014299	-8.0076	-0.10165	0.003582
-6.9988	-0.072397	0.014297	-7.0388	-0.065983	0.003582
-6.0106	-0.033116	0.014296	-6.0041	-0.021154	0.003581
-5.0066	-0.007606	0.014296	-4.985	0.009886	0.003581
-4.0493	0.011331	0.014296	-4.0239	0.030983	0.003581
-3.0511	0.040217	0.014296	-3.0337	0.060712	0.003581
-2.0048	0.067613	0.014297	-2.0111	0.090624	0.003582
-0.96264	0.099134	0.014299	-0.95983	0.12753	0.003583
0.049681	0.1259	0.014301	0.048853	0.16215	0.003583
0.96074	0.17238	0.014305	0.96811	0.19533	0.003584
2.0036	0.21683	0.014311	2.032	0.22193	0.003585
3.0221	0.24397	0.014315	3.016	0.24696	0.003586
3.9556	0.27994	0.014321	4.0643	0.27478	0.003587
4.9644	0.30282	0.014325	4.9706	0.30245	0.003589
6.016	0.3264	0.01433	6.1451	0.33191	0.00359
7.036	0.36039	0.014338	7.0374	0.35482	0.003592
8.0574	0.39897	0.014347	7.991	0.38622	0.003594
8.9579	0.41801	0.014352	8.9724	0.41565	0.003596
9.9986	0.41927	0.014353	10.023	0.44344	0.003598
11.037	0.45436	0.014363	11.044	0.45992	0.003599
12.046	0.48651	0.014373	12.04	0.47433	0.0036
12.946	0.51716	0.014382	12.959	0.49678	0.003602
14.004	0.52741	0.014386	13.994	0.51495	0.003604
15.016	0.55204	0.014395	15.023	0.53673	0.003606
16.023	0.57079	0.014401	16.03	0.55445	0.003608
16.956	0.58258	0.014406	17.032	0.57464	0.00361
17.974	0.59614	0.014411	17.988	0.592	0.003612
19.02	0.60991	0.014417	18.919	0.60374	0.003614

Table 3 Table A-2: C_L vs. α plot data, 40 degree wingtip configuration

$\alpha(150k)$	$C_L(150k)$	$\delta C_L(150k)$	$\alpha(300k)$	$C_L(300k)$	$\delta C_L(300k)$
-15.009	-0.34309	0.014271	-15.054	-0.33085	0.003573
-14.018	-0.30819	0.014264	-14.003	-0.30238	0.003571
-12.962	-0.26472	0.014256	-13.018	-0.27013	0.003569
-11.993	-0.22772	0.01425	-11.942	-0.24506	0.003568
-11.048	-0.22389	0.014249	-10.933	-0.20815	0.003567
-10.001	-0.19256	0.014245	-10.022	-0.17211	0.003566
-8.9897	-0.16665	0.014242	-8.9931	-0.13321	0.003564
-7.9985	-0.118	0.014237	-7.9825	-0.098302	0.003564
-7.0083	-0.095379	0.014236	-6.919	-0.05964	0.003563
-6.0129	-0.054667	0.014234	-6.016	-0.035523	0.003563
-4.9831	-0.026916	0.014233	-4.9828	0.008034	0.003563
-3.9353	0.002744	0.014233	-3.974	0.045002	0.003563
-3.0447	0.02361	0.014233	-3.0474	0.072879	0.003563
-2.0084	0.053816	0.014234	-2.0332	0.10778	0.003564
-0.9686	0.085014	0.014235	-0.98124	0.14919	0.003565
0.017462	0.11017	0.014237	0.037068	0.18579	0.003566
0.95651	0.15937	0.014241	0.95467	0.22399	0.003567
2.0778	0.19861	0.014246	1.9862	0.25078	0.003568
3.0338	0.22108	0.014249	3.0058	0.28353	0.00357
3.9607	0.27573	0.014258	4.0559	0.31433	0.003571
4.9576	0.30278	0.014263	4.9499	0.33794	0.003573
5.9949	0.35905	0.014275	6.0411	0.37322	0.003575
7.0286	0.36991	0.014277	7.0224	0.40409	0.003577
8.0336	0.41353	0.014288	8.028	0.43083	0.003579
9.0539	0.453	0.014299	8.9617	0.46044	0.003581
9.984	0.46236	0.014302	10.007	0.47899	0.003583
11.026	0.47315	0.014305	11.023	0.49661	0.003584
12.039	0.49154	0.014311	12.037	0.51701	0.003586
13.058	0.51467	0.014319	13.067	0.5392	0.003588
13.995	0.52477	0.014322	13.975	0.55818	0.00359
15	0.53491	0.014326	15.008	0.57688	0.003592
16.053	0.55551	0.014333	16.05	0.59244	0.003594
17.061	0.5735	0.014339	17.004	0.60443	0.003595
17.966	0.59184	0.014346	17.966	0.61846	0.003597
19.022	0.60591	0.014352	19.024	0.62888	0.003599

Table 4 Table A-2: C_L vs. α plot data, 60 degree wingtip configuration

$\alpha(150k)$	$C_L(150k)$	$\delta C_L(150k)$	$\alpha(300k)$	$C_L(300k)$	$\delta C_L(300k)$
-14.949	-0.26987	0.014538	-14.951	-0.27042	0.003631
-14.034	-0.25418	0.014535	-13.958	-0.2494	0.003629
-13.012	-0.22829	0.014531	-13.018	-0.23203	0.003629
-11.993	-0.20288	0.014528	-11.988	-0.20551	0.003627
-10.968	-0.17991	0.014525	-10.998	-0.17483	0.003626
-10.036	-0.15984	0.014522	-10.067	-0.14977	0.003626
-9.0338	-0.13422	0.01452	-9.0528	-0.11744	0.003625
-7.9802	-0.11424	0.014518	-7.9806	-0.10168	0.003625
-6.9558	-0.09632	0.014517	-6.9472	-0.080122	0.003624
-5.997	-0.06583	0.014515	-5.898	-0.048318	0.003624
-5.03	-0.037071	0.014514	-5.0175	-0.021016	0.003624
-3.9754	-0.006762	0.014514	-3.9635	0.00995	0.003624
-2.97	0.023059	0.014514	-2.9914	0.03701	0.003624
-2.047	0.045996	0.014515	-2.0463	0.058634	0.003624
-1.0139	0.070368	0.014516	-1.0149	0.083245	0.003624
-0.010607	0.10158	0.014517	-0.003844	0.11149	0.003625
1.0439	0.142	0.014521	1.0439	0.14107	0.003625
2.0326	0.14728	0.014521	2.0374	0.17015	0.003626
3.0055	0.18888	0.014526	2.9485	0.19307	0.003627
4.0114	0.20479	0.014528	4.0206	0.22803	0.003628
5.0394	0.24633	0.014534	5.043	0.2543	0.003629
5.9605	0.2677	0.014538	5.9974	0.28203	0.00363
6.982	0.30349	0.014544	6.9827	0.30558	0.003632
7.998	0.32819	0.014549	7.9895	0.32778	0.003633
9.0464	0.36747	0.014558	8.9623	0.3595	0.003635
10.038	0.3944	0.014565	10.039	0.40305	0.003638
10.99	0.4137	0.01457	10.985	0.4272	0.003639
11.998	0.44968	0.014581	11.99	0.45552	0.003642
13.045	0.461	0.014584	13.044	0.48273	0.003644
13.952	0.50096	0.014597	13.959	0.50824	0.003646
14.963	0.51122	0.0146	14.962	0.53644	0.003649
15.997	0.54959	0.014613	16	0.55598	0.003651
17.037	0.57899	0.014624	17.035	0.58591	0.003654
18.054	0.60691	0.014635	18.068	0.60904	0.003656
18.981	0.62601	0.014643	18.988	0.63266	0.003659

Table 5 Table A-2: C_L vs. α plot data, front wingtip configuration

$\alpha(150k)$	$C_L(150k)$	$\delta C_L(150k)$	$\alpha(300k)$	$C_L(300k)$	$\delta C_L(300k)$
-14.98	-0.29803	0.014363	-15	-0.28301	0.00361
-13.958	-0.27137	0.014358	-13.957	-0.26307	0.003609
-12.97	-0.2333	0.014352	-12.966	-0.23235	0.003607
-12.001	-0.20417	0.014348	-12.034	-0.20506	0.003606
-10.99	-0.18527	0.014345	-10.994	-0.17455	0.003605
-9.9621	-0.16278	0.014343	-10.004	-0.14495	0.003605
-8.9838	-0.14687	0.014341	-8.925	-0.12078	0.003604
-8.0299	-0.10478	0.014338	-8.0331	-0.095275	0.003603
-7.0036	-0.093419	0.014337	-6.9874	-0.063225	0.003603
-5.9576	-0.061805	0.014336	-5.9557	-0.030676	0.003603
-4.9736	-0.034953	0.014335	-4.9468	-0.001973	0.003603
-4.0088	-0.007121	0.014334	-4.0223	0.021452	0.003603
-2.9736	0.012307	0.014334	-2.9805	0.047202	0.003603
-2.0095	0.038284	0.014335	-2.0032	0.077398	0.003603
-1.0292	0.093825	0.014337	-1.0234	0.11438	0.003604
-0.018858	0.13612	0.01434	-0.030039	0.14164	0.003604
1.0055	0.16996	0.014344	1.0045	0.16645	0.003605
2.0015	0.18013	0.014345	2.0672	0.19292	0.003606
3.0064	0.20021	0.014347	2.9963	0.21713	0.003607
3.9796	0.23805	0.014353	3.9819	0.25238	0.003608
5.0171	0.26861	0.014358	5.0118	0.27876	0.003609
6.0409	0.30684	0.014365	6.0243	0.3098	0.003611
6.9554	0.315	0.014367	6.9649	0.3364	0.003612
8.0496	0.36826	0.014378	7.9879	0.36782	0.003614
9.0204	0.38629	0.014383	9.0298	0.39625	0.003616
10.041	0.40202	0.014387	10.018	0.42401	0.003618
11.005	0.43489	0.014396	11.015	0.45277	0.00362
11.964	0.46611	0.014405	11.974	0.47901	0.003622
13.003	0.49002	0.014412	12.992	0.50202	0.003625
14.038	0.50421	0.014417	14.046	0.52612	0.003627
14.961	0.53664	0.014428	14.985	0.54618	0.003629
15.971	0.55129	0.014433	15.963	0.5711	0.003631
16.998	0.57415	0.014442	17.02	0.5969	0.003634
18.045	0.5986	0.014451	18.039	0.62072	0.003637
18.977	0.61424	0.014457	19.01	0.65329	0.003641

Table 6 Table A-2: C_L vs. α plot data, middle wingtip configuration

$\alpha(150k)$	$C_L(150k)$	$\delta C_L(150k)$	$\alpha(300k)$	$C_L(300k)$	$\delta C_L(300k)$
-14.976	-0.30566	0.014411	-14.952	-0.27752	0.003609
-13.95	-0.28643	0.014407	-14.058	-0.24349	0.003608
-13.02	-0.24422	0.0144	-13.024	-0.22104	0.003607
-12.005	-0.20941	0.014395	-12.02	-0.19474	0.003606
-10.958	-0.17868	0.014391	-10.953	-0.16753	0.003605
-9.992	-0.16685	0.01439	-9.9784	-0.13925	0.003604
-9.0368	-0.13812	0.014387	-9.0117	-0.11186	0.003603
-7.99	-0.11123	0.014385	-7.9922	-0.085896	0.003603
-6.958	-0.085484	0.014383	-6.9686	-0.052752	0.003603
-6.0405	-0.057663	0.014382	-6.0511	-0.026344	0.003602
-5.019	-0.030221	0.014381	-5.0215	0.001469	0.003602
-3.9888	-0.010929	0.014381	-4.0002	0.024727	0.003602
-2.9739	0.017342	0.014381	-2.995	0.059305	0.003603
-1.9579	0.042794	0.014381	-2.0545	0.089953	0.003603
-1.0178	0.060453	0.014382	-1.0123	0.11545	0.003603
0.008411	0.090212	0.014383	0.007845	0.14095	0.003604
1.0395	0.11575	0.014385	1.0138	0.16292	0.003605
2.0069	0.1401	0.014387	1.9768	0.18577	0.003605
2.9782	0.15977	0.014389	3.0381	0.20718	0.003606
3.9903	0.19841	0.014393	3.9978	0.23954	0.003607
5.0511	0.21773	0.014396	5.0249	0.26429	0.003608
6.0003	0.25462	0.014402	6.0445	0.28878	0.003609
6.9901	0.28383	0.014407	7.0014	0.30905	0.00361
8.0274	0.31127	0.014412	8.0247	0.33765	0.003612
9.0245	0.33677	0.014418	9.0041	0.35557	0.003613
10.013	0.35089	0.014421	9.9691	0.38143	0.003615
10.981	0.37353	0.014426	10.977	0.40341	0.003616
12.038	0.39235	0.014431	11.994	0.4303	0.003618
13.033	0.40635	0.014435	13.037	0.44849	0.00362
14.068	0.43177	0.014442	13.994	0.47182	0.003622
14.965	0.45487	0.014448	14.986	0.49061	0.003623
16.006	0.48158	0.014456	16.004	0.50595	0.003625
17.046	0.50732	0.014465	17.057	0.52577	0.003627
17.963	0.52169	0.01447	17.957	0.54528	0.003629
18.979	0.53585	0.014474	18.982	0.56296	0.003631

Table 7 Table A-2: C_L vs. α plot data, back wingtip configuration

$\alpha(150k)$	$C_L(150k)$	$\delta C_L(150k)$	$\alpha(300k)$	$C_L(300k)$	$\delta C_L(300k)$
-15.035	-0.29274	0.015007	-15.032	-0.30235	0.003758
-14.017	-0.25555	0.015	-14.036	-0.27788	0.003756
-13	-0.22043	0.014994	-13.018	-0.24328	0.003755
-11.969	-0.2067	0.014992	-11.953	-0.21305	0.003753
-10.958	-0.18158	0.014989	-10.952	-0.17881	0.003752
-10.029	-0.14897	0.014985	-10.032	-0.14857	0.003751
-8.9989	-0.11999	0.014982	-8.9944	-0.10979	0.00375
-7.9696	-0.09686	0.014981	-7.9805	-0.084799	0.00375
-7.0498	-0.073843	0.014979	-7.0429	-0.054943	0.00375
-6.0358	-0.05336	0.014979	-5.9704	-0.023919	0.003749
-5.0097	-0.027145	0.014978	-4.9966	0.003481	0.003749
-3.952	0.010305	0.014978	-4.0571	0.037567	0.003749
-2.9585	0.030287	0.014978	-2.9654	0.066609	0.00375
-2.0329	0.042564	0.014978	-2.0219	0.088738	0.00375
-0.98519	0.069674	0.014979	-0.98239	0.121	0.003751
0.028537	0.1105	0.014982	0.046832	0.15259	0.003751
0.97382	0.11305	0.014982	0.95368	0.18211	0.003752
1.9896	0.16273	0.014987	2.0442	0.21113	0.003753
2.9978	0.19675	0.014991	2.9891	0.23985	0.003754
4.0429	0.23504	0.014996	4.0409	0.26755	0.003756
4.9947	0.25935	0.015	4.9986	0.29914	0.003757
5.9793	0.28835	0.015006	5.9762	0.31981	0.003758
7.0156	0.30291	0.015009	7.0147	0.33943	0.003759
8.0038	0.3462	0.015018	7.9816	0.36873	0.003761
9.0338	0.37315	0.015025	8.9822	0.39935	0.003763
9.9676	0.39581	0.015031	9.9764	0.41933	0.003765
10.99	0.40994	0.015035	11.029	0.44523	0.003767
12.031	0.4415	0.015044	12.033	0.47865	0.00377
13.021	0.46104	0.01505	13.055	0.51201	0.003773
13.989	0.49086	0.015059	14.109	0.53164	0.003775
14.994	0.50674	0.015065	14.999	0.54981	0.003777
16.015	0.52705	0.015072	16.019	0.57185	0.003779
17.023	0.54432	0.015078	16.994	0.58839	0.003781
17.963	0.56479	0.015086	17.963	0.60822	0.003783
19.007	0.58611	0.015094	19.029	0.63355	0.003786

Table 8 Table A-2: C_L vs. α plot data, small wingtip configuration

$\alpha(150k)$	$C_L(150k)$	$\delta C_L(150k)$	$\alpha(300k)$	$C_L(300k)$	$\delta C_L(300k)$
-15.046	-0.28298	0.014958	-15.046	-0.27172	0.003695
-14.034	-0.26082	0.014954	-14.007	-0.24019	0.003694
-12.973	-0.23089	0.014949	-13.004	-0.22031	0.003693
-11.952	-0.20731	0.014945	-11.954	-0.19102	0.003691
-10.977	-0.18225	0.014942	-10.953	-0.1668	0.003691
-10	-0.15112	0.014939	-10.018	-0.1392	0.00369
-9.005	-0.13428	0.014937	-9.0003	-0.11228	0.00369
-7.9582	-0.11515	0.014935	-7.9913	-0.085154	0.003689
-7.0082	-0.092103	0.014934	-7.045	-0.054245	0.003689
-6.0145	-0.046311	0.014932	-6.0368	-0.023765	0.003688
-5.0157	-0.0252	0.014931	-4.9956	0.003467	0.003688
-3.9537	-0.000417	0.014931	-3.945	0.030964	0.003688
-2.9536	0.023397	0.014931	-2.9701	0.058069	0.003689
-2.0226	0.050853	0.014932	-2.0159	0.080091	0.003689
-0.97757	0.077452	0.014933	-0.98558	0.10315	0.003689
0.026359	0.089203	0.014934	0.040216	0.14019	0.00369
0.95708	0.12968	0.014937	1.0209	0.1677	0.003691
2.0174	0.16355	0.01494	1.973	0.18899	0.003691
2.9936	0.19381	0.014944	2.9994	0.21071	0.003692
4.0417	0.23339	0.014949	4.0491	0.24169	0.003693
5.0574	0.26024	0.014954	5.0409	0.26833	0.003694
5.9935	0.2875	0.014959	5.9811	0.29195	0.003696
7.0125	0.31293	0.014964	7.0156	0.32186	0.003697
8.0284	0.34416	0.014971	8.0335	0.34662	0.003699
8.9674	0.37493	0.014978	8.9577	0.36851	0.0037
9.9695	0.39751	0.014984	9.9685	0.39346	0.003702
11.022	0.40757	0.014987	11.014	0.41536	0.003703
12.026	0.43	0.014993	12.031	0.44334	0.003706
13.05	0.46687	0.015005	13.04	0.46835	0.003708
13.991	0.48712	0.015011	13.973	0.48843	0.003709
14.993	0.51077	0.015019	14.999	0.51221	0.003712
15.999	0.53002	0.015026	16.043	0.53299	0.003714
16.967	0.54118	0.01503	17.06	0.54822	0.003715
17.952	0.55691	0.015036	17.957	0.56783	0.003717
19.016	0.57388	0.015042	19.021	0.58381	0.003719

Table 9 Table A-2: C_L vs. α plot data, medium wingtip configuration

$\alpha(150k)$	$C_L(150k)$	$\delta C_L(150k)$	$\alpha(300k)$	$C_L(300k)$	$\delta C_L(300k)$
-14.996	-0.27961	0.014643	-14.989	-0.25899	0.003641
-14.052	-0.24622	0.014637	-14.053	-0.23447	0.00364
-13.004	-0.22431	0.014634	-12.997	-0.213	0.003639
-11.991	-0.20707	0.014631	-12.003	-0.19043	0.003638
-11.023	-0.18111	0.014628	-11.029	-0.16501	0.003637
-10.038	-0.16693	0.014626	-10.014	-0.12947	0.003636
-9.0414	-0.13731	0.014623	-8.9933	-0.10574	0.003636
-7.9649	-0.11699	0.014621	-7.9458	-0.075226	0.003635
-6.9636	-0.082766	0.014619	-6.9703	-0.052247	0.003635
-6.0153	-0.046171	0.014617	-5.9783	-0.021183	0.003635
-4.9978	-0.02515	0.014617	-4.9998	0.001652	0.003635
-3.9905	-0.008169	0.014617	-3.9525	0.03479	0.003635
-2.9904	0.01509	0.014617	-2.9763	0.055704	0.003635
-2.0279	0.044554	0.014617	-2.0043	0.08479	0.003635
-0.99073	0.068862	0.014618	-0.98829	0.11144	0.003636
0.034123	0.080646	0.014619	0.040315	0.13709	0.003636
0.98571	0.1107	0.014621	0.99945	0.16464	0.003637
1.9547	0.14317	0.014624	1.983	0.19171	0.003638
2.998	0.18571	0.014628	3.0065	0.21465	0.003639
4.0379	0.22104	0.014633	4.0024	0.23974	0.00364
4.9631	0.25215	0.014638	4.9642	0.26424	0.003641
5.9717	0.26988	0.014641	5.9727	0.29016	0.003642
7.0373	0.30116	0.014647	7.0205	0.31807	0.003643
7.9767	0.32837	0.014653	8.0413	0.34371	0.003645
9.0584	0.35657	0.014659	9.0338	0.36743	0.003646
9.9793	0.36984	0.014662	9.9869	0.38649	0.003648
11.002	0.40838	0.014672	11.007	0.40953	0.003649
12.015	0.44131	0.014681	12.002	0.43615	0.003651
12.949	0.46022	0.014687	13.049	0.45481	0.003653
13.96	0.48126	0.014694	13.943	0.47658	0.003655
15.024	0.50758	0.014702	15.013	0.50254	0.003657
16.028	0.52394	0.014708	16.03	0.51654	0.003658
17.063	0.54957	0.014717	16.984	0.54211	0.003661
18.004	0.56373	0.014722	17.977	0.56211	0.003663
19.003	0.5794	0.014728	19.001	0.57409	0.003664

Table 10 Table A-2: C_L vs. α plot data, long wingtip configuration

$\alpha(150k)$	$C_L(150k)$	$\delta C_L(150k)$	$\alpha(300k)$	$C_L(300k)$	$\delta C_L(300k)$
-14.991	-0.24273	0.013904	-14.987	-0.23196	0.003465
-14.032	-0.2178	0.0139	-14.008	-0.21659	0.003464
-12.994	-0.1853	0.013896	-12.996	-0.18989	0.003463
-11.955	-0.16032	0.013893	-12.012	-0.16876	0.003462
-10.976	-0.13492	0.013891	-10.977	-0.13881	0.003461
-10.031	-0.11692	0.01389	-9.9699	-0.11247	0.003461
-9.0093	-0.097066	0.013888	-9.0337	-0.088747	0.003461
-7.958	-0.076889	0.013887	-8.0162	-0.070472	0.00346
-6.961	-0.053337	0.013886	-7.0053	-0.049469	0.00346
-6.0305	-0.027278	0.013886	-6.0442	-0.02613	0.00346
-4.993	-0.014108	0.013885	-4.9846	0.000323	0.00346
-4.0787	-0.002942	0.013885	-4.0106	0.014882	0.00346
-2.9578	0.014663	0.013885	-3.0123	0.033999	0.00346
-2.021	0.036913	0.013886	-1.9673	0.055635	0.00346
-0.98022	0.058956	0.013886	-1.0381	0.07587	0.00346
0.049865	0.08314	0.013888	0.039287	0.10029	0.003461
0.95409	0.090148	0.013888	1.0123	0.11639	0.003461
1.9776	0.10846	0.013889	1.9506	0.13547	0.003461
3.0202	0.13043	0.013891	2.9601	0.15421	0.003462
3.936	0.16996	0.013894	3.9918	0.17308	0.003462
4.9726	0.1946	0.013897	5.0317	0.19135	0.003463
6.0355	0.2243	0.013901	6.0223	0.21371	0.003464
7.0193	0.24361	0.013904	6.9787	0.23421	0.003464
8.0352	0.26727	0.013908	8.009	0.25913	0.003465
8.9568	0.2892	0.013912	9.0449	0.28412	0.003466
9.9814	0.31242	0.013916	9.9691	0.30181	0.003467
11.024	0.32732	0.013919	10.951	0.31682	0.003468
12.042	0.35316	0.013925	11.984	0.34477	0.00347
13.052	0.38387	0.013932	13.01	0.36349	0.003471
14.005	0.40543	0.013937	14.015	0.3915	0.003473
15.006	0.41918	0.013941	14.951	0.41273	0.003474
16.035	0.4368	0.013946	15.981	0.43103	0.003475
16.946	0.46168	0.013953	17.033	0.45691	0.003478
17.968	0.48267	0.013959	17.979	0.47744	0.003479
19.039	0.50176	0.013965	18.962	0.49224	0.003481

Table 11 Table A-2: C_L vs. α plot data, no wingtip

$C_L(150k)$	$C_D(150k)$	$\delta C_L(150k)$	$\delta C_D(150k)$	$C_L(300k)$	$C_D(300k)$	$\delta C_L(300k)$	$\delta C_D(300k)$
-0.30096	0.086379	0.013843	0.013819	-0.29054	0.092618	0.003489	0.003491
-0.27078	0.064634	0.013837	0.013817	-0.25888	0.069666	0.003487	0.003489
-0.24	0.050269	0.013832	0.013816	-0.2292	0.049864	0.003486	0.003487
-0.20917	0.038364	0.013828	0.013816	-0.19264	0.03991	0.003484	0.003485
-0.17878	0.033268	0.013824	0.013815	-0.16561	0.035215	0.003483	0.003484
-0.15717	0.028097	0.013822	0.013815	-0.1352	0.030548	0.003483	0.003483
-0.12643	0.024229	0.013819	0.013815	-0.10293	0.026968	0.003482	0.003482
-0.096953	0.022438	0.013817	0.013814	-0.057636	0.025776	0.003481	0.003482
-0.071815	0.019715	0.013816	0.013814	-0.023753	0.024285	0.003481	0.003481
-0.043944	0.022036	0.013815	0.013814	0.00545	0.024093	0.003481	0.003481
-0.015061	0.021009	0.013814	0.013814	0.030378	0.023506	0.003481	0.003481
0.027024	0.01915	0.013814	0.013814	0.060247	0.023405	0.003481	0.003482
0.056059	0.0229	0.013815	0.013814	0.091055	0.024536	0.003482	0.003482
0.078113	0.021235	0.013816	0.013814	0.12456	0.026648	0.003482	0.003483
0.099795	0.02578	0.013817	0.013814	0.15779	0.029375	0.003483	0.003484
0.13075	0.026859	0.013819	0.013815	0.18341	0.032031	0.003484	0.003485
0.14975	0.029541	0.013821	0.013815	0.21531	0.03564	0.003485	0.003486
0.17913	0.032854	0.013824	0.013815	0.23917	0.039708	0.003486	0.003488
0.21572	0.035371	0.013829	0.013816	0.26898	0.04385	0.003487	0.003489
0.24748	0.042453	0.013833	0.013816	0.2965	0.04939	0.003488	0.003491
0.27819	0.047921	0.013838	0.013817	0.32132	0.055106	0.00349	0.003493
0.30046	0.052287	0.013842	0.013817	0.34501	0.062152	0.003491	0.003494
0.32563	0.061194	0.013847	0.013818	0.36881	0.068766	0.003492	0.003496
0.35902	0.069989	0.013854	0.013819	0.40008	0.078709	0.003494	0.003499
0.37736	0.075301	0.013859	0.01382	0.42056	0.084864	0.003496	0.003501
0.4095	0.088123	0.013867	0.013821	0.44685	0.093888	0.003498	0.003504
0.4388	0.095353	0.013874	0.013822	0.4724	0.10392	0.0035	0.003506
0.46805	0.10101	0.013883	0.013823	0.49199	0.11133	0.003501	0.003508
0.47857	0.11	0.013886	0.013824	0.51295	0.12102	0.003503	0.003511
0.49151	0.12073	0.01389	0.013825	0.53434	0.13178	0.003505	0.003514
0.50653	0.12727	0.013895	0.013826	0.54922	0.14013	0.003507	0.003515
0.52979	0.14039	0.013902	0.013828	0.56641	0.14991	0.003509	0.003518
0.54687	0.14963	0.013908	0.013829	0.58126	0.1604	0.003511	0.00352
0.55892	0.15936	0.013912	0.013831	0.59612	0.16922	0.003512	0.003522
0.57731	0.1711	0.013919	0.013832	0.61608	0.1815	0.003514	0.003525

Table 12 Table A-3: C_L vs. C_D plot data, 20 degree wingtip configuration

$C_L(150k)$	$C_D(150k)$	$\delta C_L(150k)$	$\delta C_D(150k)$	$C_L(300k)$	$C_D(300k)$	$\delta C_L(300k)$	$\delta C_D(300k)$
-0.32247	0.092555	0.01433	0.014301	-0.30959	0.096567	0.00359	0.003592
-0.29747	0.078393	0.014325	0.0143	-0.28591	0.080017	0.003588	0.00359
-0.24669	0.051765	0.014315	0.014298	-0.24321	0.052646	0.003586	0.003588
-0.22018	0.045501	0.014311	0.014298	-0.22055	0.043489	0.003585	0.003586
-0.20881	0.03534	0.01431	0.014297	-0.19946	0.03592	0.003584	0.003585
-0.17475	0.030937	0.014306	0.014297	-0.1653	0.030094	0.003583	0.003584
-0.14024	0.02746	0.014302	0.014296	-0.12749	0.026273	0.003583	0.003583
-0.093226	0.026237	0.014299	0.014296	-0.10165	0.023617	0.003582	0.003582
-0.072397	0.022323	0.014297	0.014296	-0.065983	0.020564	0.003582	0.003582
-0.033116	0.01935	0.014296	0.014296	-0.021154	0.019435	0.003581	0.003581
-0.007606	0.021864	0.014296	0.014296	0.009886	0.019319	0.003581	0.003581
0.011331	0.021975	0.014296	0.014296	0.030983	0.018734	0.003581	0.003581
0.040217	0.017828	0.014296	0.014296	0.060712	0.018629	0.003581	0.003582
0.067613	0.022611	0.014297	0.014296	0.090624	0.020621	0.003582	0.003582
0.099134	0.023714	0.014299	0.014296	0.12753	0.022761	0.003583	0.003583
0.1259	0.024991	0.014301	0.014296	0.16215	0.024771	0.003583	0.003584
0.17238	0.029754	0.014305	0.014297	0.19533	0.028518	0.003584	0.003585
0.21683	0.033698	0.014311	0.014297	0.22193	0.033385	0.003585	0.003586
0.24397	0.040629	0.014315	0.014298	0.24696	0.038109	0.003586	0.003588
0.27994	0.046637	0.014321	0.014299	0.27478	0.042819	0.003587	0.003589
0.30282	0.052265	0.014325	0.014299	0.30245	0.049372	0.003589	0.003591
0.3264	0.063025	0.01433	0.0143	0.33191	0.057016	0.00359	0.003593
0.36039	0.06578	0.014338	0.014301	0.35482	0.061869	0.003592	0.003595
0.39897	0.073562	0.014347	0.014302	0.38622	0.069276	0.003594	0.003597
0.41801	0.07995	0.014352	0.014302	0.41565	0.078868	0.003596	0.0036
0.41927	0.088913	0.014353	0.014303	0.44344	0.08839	0.003598	0.003603
0.45436	0.10264	0.014363	0.014305	0.45992	0.096524	0.003599	0.003604
0.48651	0.11099	0.014373	0.014306	0.47433	0.1054	0.0036	0.003606
0.51716	0.11971	0.014382	0.014307	0.49678	0.11299	0.003602	0.003608
0.52741	0.13055	0.014386	0.014309	0.51495	0.12355	0.003604	0.00361
0.55204	0.14085	0.014395	0.01431	0.53673	0.13458	0.003606	0.003613
0.57079	0.14929	0.014401	0.014312	0.55445	0.14442	0.003608	0.003615
0.58258	0.15637	0.014406	0.014313	0.57464	0.15544	0.00361	0.003618
0.59614	0.16749	0.014411	0.014314	0.592	0.16621	0.003612	0.00362
0.60991	0.17479	0.014417	0.014316	0.60374	0.17472	0.003614	0.003622

Table 13 Table A-3: C_L vs. C_D plot data, 40 degree wingtip configuration

$C_L(150k)$	$C_D(150k)$	$\delta C_L(150k)$	$\delta C_D(150k)$	$C_L(300k)$	$C_D(300k)$	$\delta C_L(300k)$	$\delta C_D(300k)$
-0.34309	0.10928	0.014271	0.01424	-0.33085	0.10611	0.003573	0.003576
-0.30819	0.088629	0.014264	0.014238	-0.30238	0.08605	0.003571	0.003573
-0.26472	0.064736	0.014256	0.014236	-0.27013	0.060265	0.003569	0.003571
-0.22772	0.051523	0.01425	0.014235	-0.24506	0.048126	0.003568	0.00357
-0.22389	0.046913	0.014249	0.014235	-0.20815	0.038877	0.003567	0.003568
-0.19256	0.042077	0.014245	0.014235	-0.17211	0.033757	0.003566	0.003566
-0.16665	0.034015	0.014242	0.014234	-0.13321	0.02825	0.003564	0.003565
-0.118	0.028292	0.014237	0.014234	-0.098302	0.025422	0.003564	0.003564
-0.095379	0.028299	0.014236	0.014233	-0.05964	0.022955	0.003563	0.003563
-0.054667	0.028127	0.014234	0.014233	-0.035523	0.02148	0.003563	0.003563
-0.026916	0.021672	0.014233	0.014233	0.008034	0.019213	0.003563	0.003563
0.002744	0.023888	0.014233	0.014233	0.045002	0.01926	0.003563	0.003563
0.02361	0.029465	0.014233	0.014233	0.072879	0.020907	0.003563	0.003564
0.053816	0.021095	0.014234	0.014233	0.10778	0.020871	0.003564	0.003564
0.085014	0.026358	0.014235	0.014233	0.14919	0.024998	0.003565	0.003565
0.11017	0.023569	0.014237	0.014233	0.18579	0.027347	0.003566	0.003567
0.15937	0.030553	0.014241	0.014234	0.22399	0.031593	0.003567	0.003568
0.19861	0.037631	0.014246	0.014234	0.25078	0.03655	0.003568	0.00357
0.22108	0.044632	0.014249	0.014235	0.28353	0.041526	0.00357	0.003572
0.27573	0.050225	0.014258	0.014236	0.31433	0.048317	0.003571	0.003574
0.30278	0.049205	0.014263	0.014236	0.33794	0.053182	0.003573	0.003575
0.35905	0.063002	0.014275	0.014238	0.37322	0.061722	0.003575	0.003578
0.36991	0.075229	0.014277	0.014238	0.40409	0.070313	0.003577	0.003581
0.41353	0.077754	0.014288	0.014239	0.43083	0.079263	0.003579	0.003583
0.453	0.091083	0.014299	0.014241	0.46044	0.08775	0.003581	0.003586
0.46236	0.10138	0.014302	0.014242	0.47899	0.09736	0.003583	0.003588
0.47315	0.11191	0.014305	0.014243	0.49661	0.10612	0.003584	0.00359
0.49154	0.11813	0.014311	0.014244	0.51701	0.11649	0.003586	0.003593
0.51467	0.12337	0.014319	0.014245	0.5392	0.1252	0.003588	0.003595
0.52477	0.13169	0.014322	0.014246	0.55818	0.13509	0.00359	0.003598
0.53491	0.14318	0.014326	0.014247	0.57688	0.14803	0.003592	0.0036
0.55551	0.15101	0.014333	0.014249	0.59244	0.15636	0.003594	0.003602
0.5735	0.15931	0.014339	0.01425	0.60443	0.16572	0.003595	0.003604
0.59184	0.1753	0.014346	0.014252	0.61846	0.17768	0.003597	0.003606
0.60591	0.18101	0.014352	0.014253	0.62888	0.1882	0.003599	0.003608

Table 14 Table A-3: C_L vs. C_D plot data, 60 degree wingtip configuration

$C_L(150k)$	$C_D(150k)$	$\delta C_L(150k)$	$\delta C_D(150k)$	$C_L(300k)$	$C_D(300k)$	$\delta C_L(300k)$	$\delta C_D(300k)$
-0.26987	0.093608	0.014538	0.014519	-0.27042	0.098642	0.003631	0.003632
-0.25418	0.07964	0.014535	0.014518	-0.2494	0.082464	0.003629	0.003631
-0.22829	0.061193	0.014531	0.014517	-0.23203	0.065151	0.003629	0.00363
-0.20288	0.044758	0.014528	0.014516	-0.20551	0.043201	0.003627	0.003628
-0.17991	0.039274	0.014525	0.014515	-0.17483	0.035402	0.003626	0.003627
-0.15984	0.032605	0.014522	0.014515	-0.14977	0.030743	0.003626	0.003626
-0.13422	0.031829	0.01452	0.014515	-0.11744	0.027418	0.003625	0.003625
-0.11424	0.027546	0.014518	0.014515	-0.10168	0.025772	0.003625	0.003625
-0.09632	0.02607	0.014517	0.014514	-0.080122	0.023704	0.003624	0.003624
-0.06583	0.027296	0.014515	0.014514	-0.048318	0.022161	0.003624	0.003624
-0.037071	0.023489	0.014514	0.014514	-0.021016	0.020682	0.003624	0.003624
-0.006762	0.022785	0.014514	0.014514	0.00995	0.021294	0.003624	0.003624
0.023059	0.023341	0.014514	0.014514	0.03701	0.020548	0.003624	0.003624
0.045996	0.028046	0.014515	0.014514	0.058634	0.021515	0.003624	0.003624
0.070368	0.027005	0.014516	0.014514	0.083245	0.022201	0.003624	0.003624
0.10158	0.027203	0.014517	0.014514	0.11149	0.023868	0.003625	0.003625
0.142	0.028865	0.014521	0.014515	0.14107	0.025359	0.003625	0.003626
0.14728	0.033975	0.014521	0.014515	0.17015	0.028437	0.003626	0.003627
0.18888	0.04109	0.014526	0.014515	0.19307	0.031645	0.003627	0.003628
0.20479	0.044737	0.014528	0.014516	0.22803	0.035876	0.003628	0.003629
0.24633	0.047484	0.014534	0.014516	0.2543	0.041374	0.003629	0.003631
0.2677	0.052489	0.014538	0.014517	0.28203	0.045567	0.00363	0.003632
0.30349	0.058124	0.014544	0.014517	0.30558	0.051703	0.003632	0.003634
0.32819	0.062496	0.014549	0.014518	0.32778	0.056905	0.003633	0.003635
0.36747	0.069507	0.014558	0.014519	0.3595	0.064054	0.003635	0.003638
0.3944	0.075791	0.014565	0.01452	0.40305	0.072376	0.003638	0.003641
0.4137	0.081101	0.01457	0.014521	0.4272	0.079147	0.003639	0.003643
0.44968	0.08834	0.014581	0.014522	0.45552	0.087811	0.003642	0.003646
0.461	0.099975	0.014584	0.014523	0.48273	0.098327	0.003644	0.003649
0.50096	0.10988	0.014597	0.014525	0.50824	0.1065	0.003646	0.003652
0.51122	0.12077	0.0146	0.014526	0.53644	0.11658	0.003649	0.003655
0.54959	0.13413	0.014613	0.014528	0.55598	0.12801	0.003651	0.003657
0.57899	0.14577	0.014624	0.01453	0.58591	0.14045	0.003654	0.003661
0.60691	0.15405	0.014635	0.014531	0.60904	0.152	0.003656	0.003664
0.62601	0.16487	0.014643	0.014533	0.63266	0.16541	0.003659	0.003668

Table 15 Table A-3: C_L vs. C_D plot data, front wingtip configuration

$C_L(150k)$	$C_D(150k)$	$\delta C_L(150k)$	$\delta C_D(150k)$	$C_L(300k)$	$C_D(300k)$	$\delta C_L(300k)$	$\delta C_D(300k)$
-0.29803	0.1018	0.014363	0.01434	-0.28301	0.095369	0.00361	0.003612
-0.27137	0.077699	0.014358	0.014338	-0.26307	0.076231	0.003609	0.00361
-0.2333	0.057011	0.014352	0.014337	-0.23235	0.051459	0.003607	0.003609
-0.20417	0.047469	0.014348	0.014336	-0.20506	0.04194	0.003606	0.003607
-0.18527	0.041223	0.014345	0.014336	-0.17455	0.035384	0.003605	0.003606
-0.16278	0.038453	0.014343	0.014335	-0.14495	0.031262	0.003605	0.003605
-0.14687	0.029338	0.014341	0.014335	-0.12078	0.026125	0.003604	0.003604
-0.10478	0.030469	0.014338	0.014335	-0.095275	0.024028	0.003603	0.003604
-0.093419	0.028201	0.014337	0.014335	-0.063225	0.022748	0.003603	0.003603
-0.061805	0.025928	0.014336	0.014335	-0.030676	0.020665	0.003603	0.003603
-0.034953	0.024937	0.014335	0.014334	-0.001973	0.019982	0.003603	0.003603
-0.007121	0.026784	0.014334	0.014334	0.021452	0.019465	0.003603	0.003603
0.012307	0.020649	0.014334	0.014334	0.047202	0.018548	0.003603	0.003603
0.038284	0.021096	0.014335	0.014334	0.077398	0.019725	0.003603	0.003603
0.093825	0.02407	0.014337	0.014335	0.11438	0.021948	0.003604	0.003604
0.13612	0.020509	0.01434	0.014335	0.14164	0.023551	0.003604	0.003605
0.16996	0.024457	0.014344	0.014335	0.16645	0.026329	0.003605	0.003606
0.18013	0.031034	0.014345	0.014335	0.19292	0.029711	0.003606	0.003607
0.20021	0.036297	0.014347	0.014336	0.21713	0.033532	0.003607	0.003608
0.23805	0.042131	0.014353	0.014336	0.25238	0.038766	0.003608	0.00361
0.26861	0.048484	0.014358	0.014337	0.27876	0.044604	0.003609	0.003611
0.30684	0.054342	0.014365	0.014338	0.3098	0.049708	0.003611	0.003613
0.315	0.057151	0.014367	0.014338	0.3364	0.05568	0.003612	0.003615
0.36826	0.068554	0.014378	0.014339	0.36782	0.063419	0.003614	0.003617
0.38629	0.073494	0.014383	0.01434	0.39625	0.073096	0.003616	0.00362
0.40202	0.07932	0.014387	0.014341	0.42401	0.08167	0.003618	0.003622
0.43489	0.089399	0.014396	0.014342	0.45277	0.090283	0.00362	0.003625
0.46611	0.099601	0.014405	0.014343	0.47901	0.099663	0.003622	0.003628
0.49002	0.11041	0.014412	0.014345	0.50202	0.10958	0.003625	0.00363
0.50421	0.12136	0.014417	0.014346	0.52612	0.12158	0.003627	0.003633
0.53664	0.13344	0.014428	0.014348	0.54618	0.12951	0.003629	0.003635
0.55129	0.14519	0.014433	0.014349	0.5711	0.14223	0.003631	0.003639
0.57415	0.15459	0.014442	0.014351	0.5969	0.15352	0.003634	0.003642
0.5986	0.17335	0.014451	0.014354	0.62072	0.16787	0.003637	0.003645
0.61424	0.17814	0.014457	0.014355	0.65329	0.18138	0.003641	0.00365

Table 16 Table A-3: C_L vs. C_D plot data, middle wingtip configuration

$C_L(150k)$	$C_D(150k)$	$\delta C_L(150k)$	$\delta C_D(150k)$	$C_L(300k)$	$C_D(300k)$	$\delta C_L(300k)$	$\delta C_D(300k)$
-0.30566	0.092313	0.014411	0.014386	-0.27752	0.089485	0.003609	0.003611
-0.28643	0.082511	0.014407	0.014385	-0.24349	0.06372	0.003608	0.003609
-0.24422	0.059595	0.0144	0.014383	-0.22104	0.047353	0.003607	0.003608
-0.20941	0.043641	0.014395	0.014382	-0.19474	0.036708	0.003606	0.003606
-0.17868	0.039489	0.014391	0.014382	-0.16753	0.031589	0.003605	0.003605
-0.16685	0.02922	0.01439	0.014382	-0.13925	0.026995	0.003604	0.003604
-0.13812	0.027878	0.014387	0.014381	-0.11186	0.024786	0.003603	0.003604
-0.11123	0.031244	0.014385	0.014381	-0.085896	0.022398	0.003603	0.003603
-0.085484	0.025713	0.014383	0.014381	-0.052752	0.019956	0.003603	0.003603
-0.057663	0.024385	0.014382	0.014381	-0.026344	0.018559	0.003602	0.003602
-0.030221	0.022637	0.014381	0.014381	0.001469	0.018544	0.003602	0.003602
-0.010929	0.025915	0.014381	0.014381	0.024727	0.019092	0.003602	0.003602
0.017342	0.021374	0.014381	0.014381	0.059305	0.018282	0.003603	0.003603
0.042794	0.02826	0.014381	0.014381	0.089953	0.020236	0.003603	0.003603
0.060453	0.029775	0.014382	0.014381	0.11545	0.023561	0.003603	0.003604
0.090212	0.031482	0.014383	0.014381	0.14095	0.025373	0.003604	0.003605
0.11575	0.033091	0.014385	0.014381	0.16292	0.026894	0.003605	0.003605
0.1401	0.035928	0.014387	0.014382	0.18577	0.031061	0.003605	0.003606
0.15977	0.035855	0.014389	0.014382	0.20718	0.034208	0.003606	0.003607
0.19841	0.043302	0.014393	0.014382	0.23954	0.038135	0.003607	0.003609
0.21773	0.048664	0.014396	0.014383	0.26429	0.04282	0.003608	0.00361
0.25462	0.053934	0.014402	0.014383	0.28878	0.048462	0.003609	0.003611
0.28383	0.061988	0.014407	0.014384	0.30905	0.054855	0.00361	0.003613
0.31127	0.068651	0.014412	0.014385	0.33765	0.061225	0.003612	0.003615
0.33677	0.073823	0.014418	0.014385	0.35557	0.067455	0.003613	0.003616
0.35089	0.081671	0.014421	0.014386	0.38143	0.074127	0.003615	0.003618
0.37353	0.088429	0.014426	0.014387	0.40341	0.082507	0.003616	0.00362
0.39235	0.098277	0.014431	0.014388	0.4303	0.089128	0.003618	0.003622
0.40635	0.10006	0.014435	0.014388	0.44849	0.097285	0.00362	0.003624
0.43177	0.11274	0.014442	0.01439	0.47182	0.10507	0.003622	0.003627
0.45487	0.12301	0.014448	0.014391	0.49061	0.11401	0.003623	0.003629
0.48158	0.13266	0.014456	0.014392	0.50595	0.12198	0.003625	0.003631
0.50732	0.14015	0.014465	0.014394	0.52577	0.13151	0.003627	0.003633
0.52169	0.1487	0.01447	0.014395	0.54528	0.14003	0.003629	0.003635
0.53585	0.15644	0.014474	0.014396	0.56296	0.15148	0.003631	0.003638

Table 17 Table A-3: C_L vs. C_D plot data, back wingtip configuration

$C_L(150k)$	$C_D(150k)$	$\delta C_L(150k)$	$\delta C_D(150k)$	$C_L(300k)$	$C_D(300k)$	$\delta C_L(300k)$	$\delta C_D(300k)$
-0.29274	0.09671	0.015007	0.014983	-0.30235	0.095208	0.003758	0.003759
-0.25555	0.071378	0.015	0.014981	-0.27788	0.073106	0.003756	0.003758
-0.22043	0.061148	0.014994	0.01498	-0.24328	0.049664	0.003755	0.003756
-0.2067	0.051405	0.014992	0.01498	-0.21305	0.040574	0.003753	0.003754
-0.18158	0.044963	0.014989	0.014979	-0.17881	0.03362	0.003752	0.003753
-0.14897	0.036178	0.014985	0.014979	-0.14857	0.029598	0.003751	0.003752
-0.11999	0.031017	0.014982	0.014978	-0.10979	0.025377	0.00375	0.003751
-0.09686	0.028098	0.014981	0.014978	-0.084799	0.022669	0.00375	0.00375
-0.073843	0.027247	0.014979	0.014978	-0.054943	0.020964	0.00375	0.00375
-0.05336	0.022625	0.014979	0.014978	-0.023919	0.020449	0.003749	0.003749
-0.027145	0.025149	0.014978	0.014978	0.003481	0.019895	0.003749	0.003749
0.010305	0.025948	0.014978	0.014978	0.037567	0.018836	0.003749	0.003749
0.030287	0.023601	0.014978	0.014978	0.066609	0.019684	0.00375	0.00375
0.042564	0.022611	0.014978	0.014978	0.088738	0.020318	0.00375	0.00375
0.069674	0.024086	0.014979	0.014978	0.121	0.02238	0.003751	0.003751
0.1105	0.025793	0.014982	0.014978	0.15259	0.026855	0.003751	0.003752
0.11305	0.027567	0.014982	0.014978	0.18211	0.029724	0.003752	0.003753
0.16273	0.028643	0.014987	0.014979	0.21113	0.032271	0.003753	0.003754
0.19675	0.034696	0.014991	0.014979	0.23985	0.037964	0.003754	0.003755
0.23504	0.036403	0.014996	0.014979	0.26755	0.041842	0.003756	0.003757
0.25935	0.041966	0.015	0.01498	0.29914	0.046975	0.003757	0.003759
0.28835	0.048503	0.015006	0.01498	0.31981	0.052215	0.003758	0.00376
0.30291	0.051938	0.015009	0.014981	0.33943	0.05898	0.003759	0.003761
0.3462	0.062003	0.015018	0.014982	0.36873	0.065891	0.003761	0.003763
0.37315	0.071169	0.015025	0.014983	0.39935	0.071894	0.003763	0.003766
0.39581	0.071796	0.015031	0.014983	0.41933	0.078884	0.003765	0.003768
0.40994	0.086654	0.015035	0.014984	0.44523	0.089452	0.003767	0.00377
0.4415	0.10001	0.015044	0.014986	0.47865	0.10017	0.00377	0.003773
0.46104	0.10903	0.01505	0.014987	0.51201	0.10906	0.003773	0.003777
0.49086	0.11747	0.015059	0.014988	0.53164	0.12085	0.003775	0.003779
0.50674	0.12236	0.015065	0.014989	0.54981	0.12871	0.003777	0.003781
0.52705	0.13394	0.015072	0.014991	0.57185	0.13984	0.003779	0.003784
0.54432	0.14265	0.015078	0.014992	0.58839	0.15017	0.003781	0.003786
0.56479	0.14988	0.015086	0.014993	0.60822	0.16017	0.003783	0.003789
0.58611	0.16401	0.015094	0.014995	0.63355	0.17275	0.003786	0.003792

Table 18 Table A-3: C_L vs. C_D plot data, small wingtip configuration

$C_L(150k)$	$C_D(150k)$	$\delta C_L(150k)$	$\delta C_D(150k)$	$C_L(300k)$	$C_D(300k)$	$\delta C_L(300k)$	$\delta C_D(300k)$
-0.28298	0.098794	0.014958	0.014936	-0.27172	0.090229	0.003695	0.003697
-0.26082	0.076735	0.014954	0.014935	-0.24019	0.063658	0.003694	0.003695
-0.23089	0.063098	0.014949	0.014934	-0.22031	0.047549	0.003693	0.003694
-0.20731	0.055241	0.014945	0.014933	-0.19102	0.038252	0.003691	0.003692
-0.18225	0.040087	0.014942	0.014932	-0.1668	0.032537	0.003691	0.003691
-0.15112	0.035005	0.014939	0.014932	-0.1392	0.027895	0.00369	0.00369
-0.13428	0.033062	0.014937	0.014932	-0.11228	0.024162	0.00369	0.00369
-0.11515	0.028564	0.014935	0.014931	-0.085154	0.021444	0.003689	0.003689
-0.092103	0.026035	0.014934	0.014931	-0.054245	0.019343	0.003689	0.003689
-0.046311	0.02811	0.014932	0.014931	-0.023765	0.018079	0.003688	0.003688
-0.0252	0.022436	0.014931	0.014931	0.003467	0.018316	0.003688	0.003688
-0.000417	0.021952	0.014931	0.014931	0.030964	0.016755	0.003688	0.003688
0.023397	0.021347	0.014931	0.014931	0.058069	0.01806	0.003689	0.003689
0.050853	0.02271	0.014932	0.014931	0.080091	0.020356	0.003689	0.003689
0.077452	0.023178	0.014933	0.014931	0.10315	0.020523	0.003689	0.00369
0.089203	0.028547	0.014934	0.014931	0.14019	0.024004	0.00369	0.00369
0.12968	0.028083	0.014937	0.014931	0.1677	0.025874	0.003691	0.003691
0.16355	0.031745	0.01494	0.014932	0.18899	0.028635	0.003691	0.003692
0.19381	0.029065	0.014944	0.014932	0.21071	0.031417	0.003692	0.003693
0.23339	0.040652	0.014949	0.014933	0.24169	0.036947	0.003693	0.003694
0.26024	0.044506	0.014954	0.014933	0.26833	0.040171	0.003694	0.003696
0.2875	0.053696	0.014959	0.014934	0.29195	0.046611	0.003696	0.003697
0.31293	0.054967	0.014964	0.014934	0.32186	0.05287	0.003697	0.003699
0.34416	0.06192	0.014971	0.014935	0.34662	0.059499	0.003699	0.003701
0.37493	0.069764	0.014978	0.014936	0.36851	0.0667	0.0037	0.003703
0.39751	0.07776	0.014984	0.014937	0.39346	0.074497	0.003702	0.003705
0.40757	0.084736	0.014987	0.014937	0.41536	0.081913	0.003703	0.003707
0.43	0.098684	0.014993	0.014939	0.44334	0.090758	0.003706	0.003709
0.46687	0.10627	0.015005	0.01494	0.46835	0.098389	0.003708	0.003712
0.48712	0.11377	0.015011	0.014941	0.48843	0.10753	0.003709	0.003714
0.51077	0.12063	0.015019	0.014942	0.51221	0.11724	0.003712	0.003717
0.53002	0.12882	0.015026	0.014944	0.53299	0.12702	0.003714	0.003719
0.54118	0.13898	0.01503	0.014945	0.54822	0.13738	0.003715	0.003721
0.55691	0.15283	0.015036	0.014947	0.56783	0.14761	0.003717	0.003723
0.57388	0.15972	0.015042	0.014948	0.58381	0.15766	0.003719	0.003725

Table 19 Table A-3: C_L vs. C_D plot data, medium wingtip configuration

$C_L(150k)$	$C_D(150k)$	$\delta C_L(150k)$	$\delta C_D(150k)$	$C_L(300k)$	$C_D(300k)$	$\delta C_L(300k)$	$\delta C_D(300k)$
-0.27961	0.092202	0.014643	0.014622	-0.25899	0.084631	0.003641	0.003642
-0.24622	0.072223	0.014637	0.01462	-0.23447	0.065072	0.00364	0.003641
-0.22431	0.056283	0.014634	0.014619	-0.213	0.045725	0.003639	0.00364
-0.20707	0.044809	0.014631	0.014619	-0.19043	0.036421	0.003638	0.003639
-0.18111	0.035837	0.014628	0.014618	-0.16501	0.032133	0.003637	0.003638
-0.16693	0.030835	0.014626	0.014618	-0.12947	0.028158	0.003636	0.003637
-0.13731	0.026083	0.014623	0.014617	-0.10574	0.024553	0.003636	0.003636
-0.11699	0.023939	0.014621	0.014617	-0.075226	0.022868	0.003635	0.003635
-0.082766	0.020739	0.014619	0.014617	-0.052247	0.02015	0.003635	0.003635
-0.046171	0.022136	0.014617	0.014617	-0.021183	0.019194	0.003635	0.003635
-0.02515	0.023053	0.014617	0.014617	0.001652	0.01854	0.003635	0.003635
-0.008169	0.019614	0.014617	0.014617	0.03479	0.017786	0.003635	0.003635
0.01509	0.019376	0.014617	0.014617	0.055704	0.01796	0.003635	0.003635
0.044554	0.019041	0.014617	0.014617	0.08479	0.018642	0.003635	0.003636
0.068862	0.023864	0.014618	0.014617	0.11144	0.02036	0.003636	0.003636
0.080646	0.027541	0.014619	0.014617	0.13709	0.023514	0.003636	0.003637
0.1107	0.027019	0.014621	0.014617	0.16464	0.025581	0.003637	0.003638
0.14317	0.02718	0.014624	0.014618	0.19171	0.027754	0.003638	0.003639
0.18571	0.034759	0.014628	0.014618	0.21465	0.031488	0.003639	0.00364
0.22104	0.04335	0.014633	0.014619	0.23974	0.034761	0.00364	0.003641
0.25215	0.039666	0.014638	0.014619	0.26424	0.040036	0.003641	0.003642
0.26988	0.048038	0.014641	0.014619	0.29016	0.04526	0.003642	0.003644
0.30116	0.054292	0.014647	0.01462	0.31807	0.052379	0.003643	0.003646
0.32837	0.059488	0.014653	0.014621	0.34371	0.058913	0.003645	0.003648
0.35657	0.064222	0.014659	0.014621	0.36743	0.065829	0.003646	0.003649
0.36984	0.071438	0.014662	0.014622	0.38649	0.07346	0.003648	0.003651
0.40838	0.079343	0.014672	0.014623	0.40953	0.080488	0.003649	0.003653
0.44131	0.087116	0.014681	0.014624	0.43615	0.087636	0.003651	0.003655
0.46022	0.098815	0.014687	0.014626	0.45481	0.096588	0.003653	0.003657
0.48126	0.11058	0.014694	0.014627	0.47658	0.10578	0.003655	0.003659
0.50758	0.12023	0.014702	0.014628	0.50254	0.1157	0.003657	0.003662
0.52394	0.12561	0.014708	0.014629	0.51654	0.12281	0.003658	0.003664
0.54957	0.13729	0.014717	0.014631	0.54211	0.1334	0.003661	0.003667
0.56373	0.14582	0.014722	0.014632	0.56211	0.14356	0.003663	0.00367
0.5794	0.15982	0.014728	0.014634	0.57409	0.15429	0.003664	0.003671

Table 20 Table A-3: C_L vs. C_D plot data, long wingtip configuration

$C_L(150k)$	$C_D(150k)$	$\delta C_L(150k)$	$\delta C_D(150k)$	$C_L(300k)$	$C_D(300k)$	$\delta C_L(300k)$	$\delta C_D(300k)$
-0.24273	0.076587	0.013904	0.013889	-0.23196	0.074534	0.003465	0.003466
-0.2178	0.05221	0.0139	0.013888	-0.21659	0.059064	0.003464	0.003465
-0.1853	0.040494	0.013896	0.013887	-0.18989	0.040829	0.003463	0.003464
-0.16032	0.033815	0.013893	0.013886	-0.16876	0.033072	0.003462	0.003463
-0.13492	0.027374	0.013891	0.013886	-0.13881	0.027679	0.003461	0.003462
-0.11692	0.021893	0.01389	0.013886	-0.11247	0.02314	0.003461	0.003461
-0.097066	0.018651	0.013888	0.013886	-0.088747	0.02018	0.003461	0.003461
-0.076889	0.019199	0.013887	0.013886	-0.070472	0.018366	0.00346	0.00346
-0.053337	0.017804	0.013886	0.013886	-0.049469	0.017429	0.00346	0.00346
-0.027278	0.017444	0.013886	0.013885	-0.02613	0.016817	0.00346	0.00346
-0.014108	0.014265	0.013885	0.013885	0.000323	0.014619	0.00346	0.00346
-0.002942	0.015664	0.013885	0.013885	0.014882	0.014235	0.00346	0.00346
0.014663	0.014395	0.013885	0.013885	0.033999	0.014485	0.00346	0.00346
0.036913	0.015807	0.013886	0.013885	0.055635	0.01478	0.00346	0.00346
0.058956	0.014633	0.013886	0.013886	0.07587	0.014408	0.00346	0.003461
0.08314	0.020143	0.013888	0.013886	0.10029	0.017791	0.003461	0.003461
0.090148	0.019955	0.013888	0.013886	0.11639	0.019619	0.003461	0.003461
0.10846	0.021296	0.013889	0.013886	0.13547	0.022795	0.003461	0.003462
0.13043	0.026053	0.013891	0.013886	0.15421	0.024688	0.003462	0.003462
0.16996	0.028055	0.013894	0.013886	0.17308	0.028	0.003462	0.003463
0.1946	0.034234	0.013897	0.013887	0.19135	0.0322	0.003463	0.003464
0.2243	0.040898	0.013901	0.013887	0.21371	0.036361	0.003464	0.003465
0.24361	0.045473	0.013904	0.013888	0.23421	0.041254	0.003464	0.003466
0.26727	0.048552	0.013908	0.013888	0.25913	0.04596	0.003465	0.003467
0.2892	0.05225	0.013912	0.013889	0.28412	0.051706	0.003466	0.003469
0.31242	0.061463	0.013916	0.013889	0.30181	0.057872	0.003467	0.00347
0.32732	0.065091	0.013919	0.01389	0.31682	0.062446	0.003468	0.003471
0.35316	0.070918	0.013925	0.01389	0.34477	0.068124	0.00347	0.003473
0.38387	0.084841	0.013932	0.013892	0.36349	0.075752	0.003471	0.003475
0.40543	0.090521	0.013937	0.013892	0.3915	0.085118	0.003473	0.003477
0.41918	0.10207	0.013941	0.013893	0.41273	0.093577	0.003474	0.003479
0.4368	0.11164	0.013946	0.013895	0.43103	0.10215	0.003475	0.003481
0.46168	0.12083	0.013953	0.013896	0.45691	0.11232	0.003478	0.003484
0.48267	0.12879	0.013959	0.013897	0.47744	0.12172	0.003479	0.003486
0.50176	0.14475	0.013965	0.013899	0.49224	0.1323	0.003481	0.003488

Table 21 Table A-3: C_L vs. C_D plot data, no wingtip

B. Appendix B: Sample Calculations

Sample calculations shown for the 20 degree wingtip configuration, tested at an approximate Reynold number of 150,000, at a positive six degree angle of attack:

$$S = c \cdot b = 0.0213m^2$$

$$Re = 150,800$$

$$p_{atm} = 96710Pa$$

$$T = 295.45K$$

$$\rho_{\infty} = \frac{p_{atm}}{R_{air} \cdot T} = 1.14052 \frac{kg}{m^3}$$

$$\delta\rho = \sqrt{\left(\frac{1}{RT}\delta p\right)^2 + \left(\frac{p}{RT^2}\delta T\right)^2} = 0.0040364 \frac{kg}{m^3}$$

$$\mu = \mu_{ref} \left(\frac{T}{T_{ref}}\right)^{3/2} \left(\frac{T_{ref} + S_{\mu}}{T + S_{\mu}}\right) = 1.8243E^{-5} \frac{kg}{m \cdot s}$$

$$V_{\infty} = \frac{Re \cdot \mu}{\rho_{\infty} \cdot c} = 17.2662 \frac{m}{s}$$

$$q_{\infty} = \frac{1}{2} \rho_{\infty} V_{\infty}^2 = 170.0083Pa$$

$$F_{A_{test}} = 0.891832N, F_{A_{grav}} = 0.81667N$$

$$F_{N_{test}} = 1.140192N, F_{N_{grav}} = 0.038874N$$

$$F_A = 0.075162N$$

$$F_N = 1.101318N$$

$$\alpha = 5.967635^{\circ} = 0.104155rad$$

$$L = F_N \cdot \cos \alpha - F_A \cdot \sin \alpha = 1.087535N$$

$$D = F_N \cdot \sin \alpha + F_A \cdot \cos \alpha = 0.189255N$$

$$C_L = \frac{L}{q_{\infty} S} = 0.30046$$

$$C_D = \frac{D}{q_{\infty} S} = 0.052287$$

$$\delta C_L = \sqrt{\left(\frac{\partial C_L}{\partial F_A} \delta F_A\right)^2 + \left(\frac{\partial C_L}{\partial F_N} \delta F_N\right)^2 + \left(\frac{\partial C_L}{\partial \alpha} \delta \alpha\right)^2 + \left(\frac{\partial C_L}{\partial q_{\infty}} \delta q_{\infty}\right)^2} = 0.013842$$

$$\delta C_D = \sqrt{\left(\frac{\partial C_D}{\partial F_A} \delta F_A\right)^2 + \left(\frac{\partial C_D}{\partial F_N} \delta F_N\right)^2 + \left(\frac{\partial C_D}{\partial \alpha} \delta \alpha\right)^2 + \left(\frac{\partial C_D}{\partial q_{\infty}} \delta q_{\infty}\right)^2} = 0.013817$$

C. Appendix C: MATLAB Code

```
%% Header
% Author: Zakary Steenhoek
% Date: 18 November 2024
% AEE361::LAB04

clc; clear; clf; %close all;

%% Process Data

% Read all data
readData();

% To store data
allProcessedData = struct('testName', [], 'data', []);

% Loop on every test file
for itr1 = 1:1% numel(allTestData)
    % Grab filename and data
    thisTestName = lower(allTestData(itr1).filename);
    thisTestData = allTestData(itr1).data;

    % Extract file specifics
    fileSpecifics = split(thisTestName, '_');
    thisWinglet = fileSpecifics{1}; thisRe = fileSpecifics{2};

    % Get conditions for this winglet
    for whichCond = 1:length(conditions)
        if contains(thisTestName, conditions(whichCond, 1))
            theseConditions = conditions(whichCond, :);
            break
        end
    end

    % Get grav data for this winglet
    for itr = 1:length(allGravData)
        if contains(allGravData(itr).filename, thisWinglet)
            thisGravData = allGravData(itr).data;
            break
        end
    end

    % Determine which reynolds number for this winglet
    if contains(thisTestName, "150k")
        re = theseConditions{4}
    else
        re = theseConditions{5}
    end

    % Grab pressure and temp from subcell array
    pres = theseConditions{3}*1000
    temp = theseConditions{2}+273.15

    % Call to process this test file and store data
    [theseResults, rho, thisUncertainRho] = processfile(thisGravData, ...
```

```

        thisTestData, pres, temp, re);
allProcessedData(itr1).testName = thisTestName;
allProcessedData(itr1).data = theseResults;

if (theseConditions{6} == 0)
    conditions{whichCond,6} = rho
    conditions{whichCond,7} = thisUncertainRho

end
end

%% Sort Data

% To organize data
location_150 = struct('winglet', locationFam, 'data', []);
location_300 = struct('winglet', locationFam, 'data', []);
length_150 = struct('winglet', lengthFam, 'data', []);
length_300 = struct('winglet', lengthFam, 'data', []);
angle_150 = struct('winglet', angleFam, 'data', []);
angle_300 = struct('winglet', angleFam, 'data', []);
none_150 = struct('winglet', 'none', 'data', []);
none_300 = struct('winglet', 'none', 'data', []);

% Loop on every processed test
for itr2 = 1:numel(allProcessedData)
    % Break out this iteration data
    thisName = allProcessedData(itr2).testName;
    thisData = allProcessedData(itr2).data;
    sub = split(thisName, '_');

    % If this is a 150k test
    if contains(thisName, "150k")
        % If this belongs to the location family
        if contains(thisName, locationFam)
            % Determine which one
            iw = find(contains(locationFam, sub{1}),1);
            location_150(iw).data = thisData;
            % Else if this belongs to the length family
            elseif contains(thisName, lengthFam)
                iw = find(contains(lengthFam, sub{1}),1);
                length_150(iw).data = thisData;
            % Else if this belongs to the angle family
            elseif contains(thisName, angleFam)
                iw = find(contains(angleFam, sub{1}),1);
                angle_150(iw).data = thisData;
            % Else this is none
            else
                none_150.data = thisData;
            end
        % Else this is a 300k test
    else
        % If this belongs to the location family
        if contains(thisName, locationFam)
            % Determine which one
            iw = find(contains(locationFam, sub{1}),1);

```

```

        location_300(iw).data = thisData;
        % Else if this belongs to the length family
    elseif contains(thisName, lengthFam)
        iw = find(contains(lengthFam, sub{ 1 }),1);
        length_300(iw).data = thisData;
        % Else if this belongs to the angle family
    elseif contains(thisName, angleFam)
        iw = find(contains(angleFam, sub{ 1 }),1);
        angle_300(iw).data = thisData;
        % Else this is none
    else
        none_300.data = thisData;
    end
end
end

%% Plot Data

plotfamily(location_150,none_150,[1,2]);
plotfamily(length_150,none_150,[3,4]);
plotfamily(angle_150,none_150,[5,6]);

% plotfamily(location_300,none_300,[7,8]);
% plotfamily(length_300,none_300,[9,10]);
% plotfamily(angle_300,none_300,[11,12]);

%% Export Data

% % Open a file to write
% fileID = fopen('processed_data.csv', 'w');
%
% % Write data for each struct entry
% for i = 1:numel(allProcessedData)
%     % Write the test name
%     fprintf(fileID, '%s\n', allProcessedData(i).testName{ 1 });
%
%     % Write the data array
%     fprintf(fileID, '%.6f,%.6f,%.6f,%.6f,%.6f\n', allProcessedData(i).data');
%     fprintf(fileID, '\n');
% end
%
% % Close the file
% fclose(fileID);

%% Header
% Author: Zakary Steenhoek
% Date: 18 November 2024
% Title: readData
% Description: This
% AEE361::LAB04

%% References

% Explicit paths to data
dataPath = "C:\Users\zaste\OneDrive\Documents\Software\MATLAB\AEE360\Lab-4\data\best";

```

```

unneededVars = {'Type','Units','Time','Humidity','Temperature','BarometricPressure'};

locationFam = {'front','mid','back'};
lengthFam = {'small','med','long'};
angleFam = {'20deg','40deg','60deg'};

conditionsFile = strcat(dataPath, "Lab4_G6_Conditions.txt");
gravFiles = dir(strcat(dataPath, "grav\*.csv"));
testFiles = dir(strcat(dataPath, "test\*.csv"));

% conditionsFile = strcat(dataPath1, "Lab4_G7_Conditions.txt");
% files = dir(strcat(dataPath1, "*.csv"));

%% Read and refine Data

% Organize data into structs. Field one for name, field 2 for data
allGravData = struct();
allTestData = struct();

% Read conditions file as table and convert to cell array
conditions = table2cell(readtable(conditionsFile));
conditions(:,1) = lower(conditions(:,1));
conditions(:,6:7) = {0};

% Loop on grav files
for i = 1:numel(gravFiles)
    % Check only grav files
    if contains(gravFiles(i).name, 'grav', 'IgnoreCase',true)

        % Split file name and homogenize for clarity
        [~,name,~] = fileparts(gravFiles(i).name);
        nameParts = lower(split(name, '_'));
        if contains(nameParts(end-1), {'20','40','60'})
            if ~contains(nameParts(end-1), 'deg')
                nameParts(end-1) = strcat(nameParts(end-1),'deg');
            end
        end
        allGravData(i).filename = join(nameParts(end-1:end), '_');

        % Read data into a table and remove unneeded columns
        fileData = readtable(gravFiles(i).name);
        fileData = removevars(fileData,unneededVars);

        % Convert to cell array and concat with column headings
        allGravData(i).data = table2array(fileData);
    end
end

% Loop on test files
for i = 1:numel(testFiles)
    % Check only test files
    if ~contains(testFiles(i).name, 'grav', 'IgnoreCase',true)

        % Split file name and homogenize for clarity
        [~,name,~] = fileparts(testFiles(i).name);
        nameParts = lower(split(name, '_'));
    end
end

```



```

        if contains(nameParts(end-1), {'20','40','60'})
            if ~contains(nameParts(end-1), 'deg')
                nameParts(end-1) = strcat(nameParts(end-1),'deg');
            end
        end
        allTestData(i).filename = join(nameParts(end-1:end), '_');

        % Read data into a table and remove unneeded columns
        fileData = readtable(testFiles(i).name);
        fileData = removevars(fileData,unneededVars);

        % Convert to cell array and concat with column headings
        allTestData(i).data = table2array(fileData);
    end
end

% % Loop on files
% gravi = 1;
% testi = 1;
% for i = 1:numel(files)
%     % Check only grav files
%     if contains(files(i).name, 'grav', 'IgnoreCase',true)
%
%         % Split file name and homogenize for clarity
%         [~,name,~] = fileparts(files(i).name);
%         nameParts = lower(split(name, '_'));
%         allGravData(gravi).filename = join(nameParts(end-1:end), '_');
%
%         % Read data into a table and remove unneeded columns
%         fileData = readtable(files(i).name);
%         fileData = removevars(fileData,unneededVars);
%
%         % Convert to cell array and concat with column headings
%         allGravData(gravi).data = table2array(fileData);
%         gravi = gravi+1;
%     end
% end
% for i = 1:numel(files)
%     % Check only test files
%     if ~contains(files(i).name, 'grav', 'IgnoreCase',true)
%
%         % Split file name and homogenize for clarity
%         [~,name,~] = fileparts(files(i).name);
%         nameParts = lower(split(name, '_'));
%         allTestData(testi).filename = join(nameParts(end-1:end), '_');
%
%         % Read data into a table and remove unneeded columns
%         fileData = readtable(files(i).name);
%         fileData = removevars(fileData,unneededVars);
%
%         % Convert to cell array and concat with column headings
%         allTestData(testi).data = table2array(fileData);
%         testi = testi + 1;
%     end
% end

```

```

% To save my poor laptop memory
clear gravFiles testFiles fileData nameParts name i
% clear files fileData nameParts name i

%PROCESSFILE Compute lift, drag, lift coefficient, drag coefficient from
% these specific files. Store the data sensibly and return it.

function [results,rho,uncertainRho] = processfile(gravdata,testdata,pressure,temperature,renum)
% Constants
R_AIR = 287.0;
MU_REF = 1.716e-5;
S_MU = 110.4;
T_REF = 273.15;
CHORD = 0.1397;
SPAN = 0.1524;
PLANFORM = CHORD*SPAN;
ERR_F = 0.05;
ERR_PITCH = 0.05;
ERR_QINF = 0.5;
ERR_THERMO = 1;
ERR_ABS_TRANSDUCER = 100;

% Inline functions
gasLaw_rho = @(P,T) P./(R_AIR.*T);
sutherland = @(T) MU_REF*(T/T_REF)^1.5*((T_REF+S_MU)/(T+S_MU));
reynold_vel = @(RE,MU,RHO) (RE*MU)/(RHO*CHORD);
pDyn = @(V,RHO) 0.5.*RHO.*V.^2;

% Air density uncertainty due to machine error
d_RHO_P = @(T) 1./(R_AIR.*T);
d_RHO_T = @(P,T) -P./(R_AIR.*T.^2);

% Derivatives
d_CL_N = @(P,Q) cos(P)./(Q.*PLANFORM);
d_CL_A = @(P,Q) -sin(P)./(Q.*PLANFORM);
d_CL_P = @(P,Q,A,N) -(A.*cos(P) + N.*sin(P))./(Q.*PLANFORM);
d_CL_Q = @(P,Q,A,N) -(N.*cos(P) - A.*sin(P))./(Q.^2.*PLANFORM);

d_CD_N = @(P,Q) sin(P)./(Q.*PLANFORM);
d_CD_A = @(P,Q) cos(P)./(Q.*PLANFORM);
d_CD_P = @(P,Q,A,N) (N.*cos(P) - A.*sin(P))./(Q.*PLANFORM);
d_CD_Q = @(P,Q,A,N) -(A.*cos(P) + N.*sin(P))./(Q.^2.*PLANFORM);

% Solve equations
rho = gasLaw_rho(pressure, temperature)
mu = sutherland(temperature)
vel = reynold_vel(renum,mu,rho)
qinf = pDyn(vel, rho)

% Grab the data we actually need
gravAxial = gravdata(2:end,1); gravNormal = gravdata(2:end,2)
testAxial = testdata(2:end,1); testNormal = testdata(2:end,2)
pitchAngle = testdata(2:end,4);

% Compensate for the weight of the wing and convert pitch

```

```

totalAxial = testAxial-gravAxial;
totalNormal = testNormal-gravNormal;
alpha = deg2rad(pitchAngle);
ERR_ALPHA = deg2rad(ERR_PITCH);

% Compute values
lift = totalNormal.*cos(alpha)-totalAxial.*sin(alpha)
drag = totalNormal.*sin(alpha)+totalAxial.*cos(alpha)
coeffLift = lift./(qinf*PLANFORM)
coeffDrag = drag./(qinf*PLANFORM)

% Compute uncertainty values
uncCL_n = (d_CL_N(alpha,qinf).*ERR_F).^2
uncCL_a = (d_CL_A(alpha,qinf).*ERR_F).^2
uncCL_pitch = (d_CL_P(alpha,qinf,totalAxial,totalNormal).*ERR_ALPHA).^2
uncCL_press = (d_CL_Q(alpha,qinf,totalAxial,totalNormal).*ERR_QINF).^2
unc_CL = sqrt(uncCL_n+uncCL_a+uncCL_pitch+uncCL_press)

uncCD_n = (d_CD_N(alpha,qinf).*ERR_F).^2
uncCD_a = (d_CD_A(alpha,qinf).*ERR_F).^2
uncCD_pitch = (d_CD_P(alpha,qinf,totalAxial,totalNormal).*ERR_ALPHA).^2
uncCD_press = (d_CD_Q(alpha,qinf,totalAxial,totalNormal).*ERR_QINF).^2
unc_CD = sqrt(uncCD_n+uncCD_a+uncCD_pitch+uncCD_press)

unc_RHO_P = (d_RHO_P(temperature).*ERR_ABS_TRANSDUCER).^2
unc_RHO_T = (d_RHO_T(pressure, temperature).*ERR_THERMO).^2

% Round for consistancy
pitchAngle = round(pitchAngle, 5, "significant")
coeffLift = round(coeffLift, 5, "significant")
coeffDrag = round(coeffDrag, 5, "significant")
unc_CL = round(unc_CL, 5, "significant")
unc_CD = round(unc_CD, 5, "significant")

% Return results
results = [pitchAngle,coeffLift,coeffDrag,unc_CL,unc_CD];
uncertainRho = sqrt(unc_RHO_P+unc_RHO_T)
end

%PLOTFAMILY plots the lift curve and drag polar for a specified winglet
% family. Some args are optional and have default values

function [familydata,nonedata] = plotfamily(familydata,nonedata,figrange)
% If no custom range, default 1,2
if isempty(figrange)
    figrange = [1,2];
end
% Default krb line specs
famSpecs = {'k.-','b.-','r.-'};
noneSpec = 'k.-';
% famSpecs = {'r.-','g.-','b.-'};
% noneSpec = 'k.-';

figDir = ['C:\Users\zaste\OneDrive\Documents\Software\MATLAB\AEE360\' ...
    'Lab-4\figures\best\krbk-'];

```

```

% Get and parse name
famName = inputname(1);
parts = split(famName, '_');
fam = parts{1};
rey = parts{2};
subtitle = {strjoin({'Winglet family:', fam}, ' '), ...
    strcat(strjoin({'Approx. reynold number:', rey}, ' '), 'k')};

% Lift slope
figure(figure(1)); clf; hold on; grid on;
title('Lift Coefficient vs. Pitch Angle', subtitle);
xlabel('Pitch angle (deg)'); ylabel('Lift Coefficient (dimless)');
errorbar(nonedata.data(:,1), nonedata.data(:,2), nonedata.data(:,4), noneSpec)
for i = 1:3
    errorbar(familydata(i).data(:,1), familydata(i).data(:,2), ...
        familydata(i).data(:,4), famSpecs{i});
end
legend(nonedata.winglet, familydata(1).winglet, familydata(2).winglet, ...
    familydata(3).winglet, 'Location', 'best');
xlim([-15 20]); ylim([-0.4 0.8]);
hold off;

q = findobj('type', 'figure');
figTitle = strjoin({'Lab4_liftslope', famName}, '_');
% autosave(q, figTitle, figDir, 'png', false)

% Drag polar
figure(figure(2)); clf; hold on; grid on;
title('Drag Polar', subtitle);
xlabel('Drag Coefficient (dimless)'); ylabel('Lift Coefficient (dimless)');
plot(nonedata.data(:,3), nonedata.data(:,2), noneSpec);
% errorbar(nonedata.data(:,3), nonedata.data(:,2), nonedata.data(:,4)./2, ...
% nonedata.data(:,4)./2, nonedata.data(:,5)./2, nonedata.data(:,5)./2, noneSpec)
for i = 1:3
    plot(familydata(i).data(:,3), familydata(i).data(:,2), famSpecs{i});
    % errorbar(familydata(i).data(:,3), familydata(i).data(:,2), ...
    % familydata(i).data(:,4)./2, familydata(i).data(:,4)./2, ...
    % familydata(i).data(:,5)./2, familydata(i).data(:,5)./2, famSpecs{i});
end
legend(nonedata.winglet, familydata(1).winglet, familydata(2).winglet, ...
    familydata(3).winglet, 'Location', 'best');
xlim([0 0.2]); ylim([-0.4 0.8]);
hold off;

q = findobj('type', 'figure');
figTitle = strjoin({'Lab4_dragpolar', famName}, '_');
% autosave(q, figTitle, figDir, 'png', false)
end

%% temp math
clear; clc;

sympref('FloatingPointOutput', true);
syms N A Q P S R T

```

$$L = N \cos(P) - A \sin(P);$$

$$D = N \sin(P) + A \cos(P);$$

$$CL = L/(Q \cdot S);$$

$$CD = D/(Q \cdot S);$$

$$d_CL_N = \text{diff}(CL, N);$$

$$d_CL_A = \text{diff}(CL, A);$$

$$d_CL_P = \text{diff}(CL, P);$$

$$d_CL_Q = \text{diff}(CL, Q);$$

$$d_CD_N = \text{diff}(CD, N);$$

$$d_CD_A = \text{diff}(CD, A);$$

$$d_CD_P = \text{diff}(CD, P);$$

$$d_CD_Q = \text{diff}(CD, Q);$$

$$d_CL_N = @(P, Q, S) \cos(P)/(Q \cdot S);$$

$$d_CL_A = @(P, Q, S) -\sin(P)/(Q \cdot S);$$

$$d_CL_P = @(A, P, N, Q, S) -(A \cos(P) + N \sin(P))/(Q \cdot S);$$

$$d_CL_Q = @(A, P, N, Q, S) -(N \cos(P) - A \sin(P))/(Q^2 \cdot S);$$

$$d_CD_N = @(P, Q, S) \sin(P)/(Q \cdot S);$$

$$d_CD_A = @(P, Q, S) \cos(P)/(Q \cdot S);$$

$$d_CD_P = @(A, P, N, Q, S) (N \cos(P) - A \sin(P))/(Q \cdot S);$$

$$d_CD_Q = @(A, P, N, Q, S) -(A \cos(P) + N \sin(P))/(Q^2 \cdot S);$$

$$\text{gasLaw_rho} = P./(R \cdot T);$$

$$d_RHO_P = \text{diff}(\text{gasLaw_rho}, P);$$

$$d_RHO_T = \text{diff}(\text{gasLaw_rho}, T);$$

D. Acknowledgments

I would first like to thank my lab TA for the beautiful figures and guidance throughout the experiment. I would also like to thank Monster Beverage Corporation for providing me with the necessary caffeine to get through this week. I just really wish they would lower their prices. Lastly, I would like to thank my cat Robby for the moral support he provided, i.e. screaming outside my door whenever I did not let him watch me do my homework and step on my keyboard.

References

- [1] AEE361, “Lab4Manual.pdf,” , 2024. URL https://canvas.asu.edu/courses/200674/files/96015161?module_item_id=15007790
- [2] munroscientificdivision, 2024. URL <https://www.munroscientific.co.uk/a-guide-for-laboratory-thermometer#:~:text=A%20laboratory%20thermometer%20is%20an, scale%20that%20indicates%20the%20temperature.>
- [3] NASA, “Pitot tube,” , 2024. URL <https://www.grc.nasa.gov/www/k-12/VirtualAero/BottleRocket/airplane/pitot.html>
- [4] Dewesoft, “What Is Data Acquisition?” , February 2024. URL <https://dewesoft.com/blog/what-is-data-acquisition>
- [5] Online, C., “Sutherland’s law,” , October 2008. URL https://www.cfd-online.com/Wiki/Sutherland%27s_law
- [6] CalculatorSoup, L., “Celsius to Kelvin: °C to K,” , Aug 2023. URL <https://www.calculatorsoup.com/calculators/conversions/celsius-to-kelvin.php>
- [7] Mathworks, 2024. URL <https://www.mathworks.com/help/matlab/>
- [8] NASA, “Low speed tunnel operation,” , 2021. URL <https://www.grc.nasa.gov/www/k-12/airplane/tunop.html>
- [9] www.convertunits.com, “Convert inH2O to pascal,” , 2024. URL <https://www.convertunits.com/from/inH20/to/pascal>
- [10] AEE361, “Machine error chart.xls,” , 2024. URL https://canvas.asu.edu/courses/200674/files/90845854?module_item_id=14598811
- [11] Horiba, “What Is a Wind Tunnel Balance?” , April 2024. URL <https://www.horiba.com/usa/company/news/detail/news/4/2024/what-is-a-wind-tunnel-balance>
- [12] AEE361-G6, “Lab4_G6_Conditions,” , November 2024. URL <https://canvas.asu.edu/courses/200674/modules/items/15066575>
- [13] AEE361-G5, “Lab4_G5_20deg_grav,” , November 2024. URL <https://canvas.asu.edu/courses/200674/modules/items/15050380>
- [14] AEE361-G5, “Lab4_G5_40deg_grav,” , November 2024. URL <https://canvas.asu.edu/courses/200674/modules/items/15055806>
- [15] AEE361-G5, “Lab4_G5_60deg_grav,” , November 2024. URL <https://canvas.asu.edu/courses/200674/modules/items/15055807>
- [16] AEE361-G5, “Lab4_G5_med_grav,” , November 2024. URL <https://canvas.asu.edu/courses/200674/modules/items/15055810>
- [17] AEE361-G5, “Lab4_G5_none_grav,” , November 2024. URL <https://canvas.asu.edu/courses/200674/modules/items/15050381>
- [18] AEE361-G6, “Lab4_G6_back_grav,” , November 2024. URL <https://canvas.asu.edu/courses/200674/modules/items/15061672>
- [19] AEE361-G6, “Lab4_G6_front_grav,” , November 2024. URL <https://canvas.asu.edu/courses/200674/modules/items/15066594>
- [20] AEE361-G6, “Lab4_G6_long_grav,” , November 2024. URL <https://canvas.asu.edu/courses/200674/modules/items/15066596>
- [21] AEE361-G6, “Lab4_G6_small_grav,” , November 2024. URL <https://canvas.asu.edu/courses/200674/modules/items/15066599>
- [22] AEE361-G7, “Lab4_G7_mid_grav,” , November 2024. URL <https://canvas.asu.edu/courses/200674/modules/items/15069335>

- [23] AEE361-G5, “Lab4_G5_20deg_150k,” , November 2024. URL <https://canvas.asu.edu/courses/200674/modules/items/15050376>.
- [24] AEE361-G5, “Lab4_G5_40deg_150k,” , November 2024. URL <https://canvas.asu.edu/courses/200674/modules/items/15055793>.
- [25] AEE361-G5, “Lab4_G5_60deg_150k,” , November 2024. URL <https://canvas.asu.edu/courses/200674/modules/items/15055795>.
- [26] AEE361-G5, “Lab4_G5_med_150k,” , November 2024. URL <https://canvas.asu.edu/courses/200674/modules/items/15055801>.
- [27] AEE361-G5, “Lab4_G5_none_150k,” , November 2024. URL <https://canvas.asu.edu/courses/200674/modules/items/15050378>.
- [28] AEE361-G6, “Lab4_G6_back_150k,” , November 2024. URL <https://canvas.asu.edu/courses/200674/modules/items/15061669>.
- [29] AEE361-G6, “Lab4_G6_front_150k,” , November 2024. URL <https://canvas.asu.edu/courses/200674/modules/items/15066579>.
- [30] AEE361-G6, “Lab4_G6_long_150k,” , November 2024. URL <https://canvas.asu.edu/courses/200674/modules/items/15066581>.
- [31] AEE361-G6, “Lab4_G6_small_150k,” , November 2024. URL <https://canvas.asu.edu/courses/200674/modules/items/15066588>.
- [32] AEE361-G7, “Lab4_G7_mid_150k,” , November 2024. URL <https://canvas.asu.edu/courses/200674/modules/items/15069327>.
- [33] AEE361-G5, “Lab4_G5_20deg_300k,” , November 2024. URL <https://canvas.asu.edu/courses/200674/modules/items/15050377>.
- [34] AEE361-G5, “Lab4_G5_40deg_300k,” , November 2024. URL <https://canvas.asu.edu/courses/200674/modules/items/15055794>.
- [35] AEE361-G5, “Lab4_G5_60deg_300k,” , November 2024. URL <https://canvas.asu.edu/courses/200674/modules/items/15055796>.
- [36] AEE361-G5, “Lab4_G5_med_300k,” , November 2024. URL <https://canvas.asu.edu/courses/200674/modules/items/15055802>.
- [37] AEE361-G5, “Lab4_G5_none_300k,” , November 2024. URL <https://canvas.asu.edu/courses/200674/modules/items/15050379>.
- [38] AEE361-G6, “Lab4_G6_back_300k,” , November 2024. URL <https://canvas.asu.edu/courses/200674/modules/items/15061670>.
- [39] AEE361-G6, “Lab4_G6_front_300k,” , November 2024. URL <https://canvas.asu.edu/courses/200674/modules/items/15066580>.
- [40] AEE361-G6, “Lab4_G6_long_300k,” , November 2024. URL <https://canvas.asu.edu/courses/200674/modules/items/15066582>.
- [41] AEE361-G6, “Lab4_G6_small_300k,” , November 2024. URL <https://canvas.asu.edu/courses/200674/modules/items/15066589>.
- [42] AEE361-G7, “Lab4_G7_mid_300k,” , November 2024. URL <https://canvas.asu.edu/courses/200674/modules/items/15069328>.